
UMA: A Family of Universal Models for Atoms

Brandon M. Wood^{1,*,\dagger} Misko Dzamba^{1,*} Xiang Fu^{1,*} Meng Gao^{1,*} Muhammed Shuaibi^{1,*}
Luis Barroso-Luque¹ Kareem Abdelmaqsoud² Vahe Gharakhanyan¹ John R. Kitchin²
Daniel S. Levine¹ Kyle Michel¹ Anuroop Sriram¹ Taco Cohen¹ Abhishek Das¹
Ammar Rizvi¹ Sushree Jagriti Sahoo¹ Zachary W. Ulissi¹ C. Lawrence Zitnick^{1,\dagger}
¹FAIR at Meta ²CMU

Abstract

The ability to quickly and accurately compute properties from atomic simulations is critical for advancing a large number of applications in chemistry and materials science including drug discovery, energy storage, and semiconductor manufacturing. To address this need, we present a family of Universal Models for Atoms (UMA), designed to push the frontier of speed, accuracy, and generalization. UMA models are trained on half a billion unique 3D atomic structures (the largest training runs to date) by compiling data across multiple chemical domains, e.g. molecules, materials, and catalysts. We develop empirical scaling laws to help understand how to increase model capacity alongside dataset size to achieve the best accuracy. The UMA small and medium models utilize a novel architectural design we refer to as mixture of linear experts that enables increasing model capacity without sacrificing speed. For example, UMA-medium has 1.4B parameters but only ~ 50 M active parameters per atomic structure. We evaluate UMA models on a diverse set of applications across multiple domains and find that, remarkably, a single model without any fine-tuning can perform similarly or better than specialized models. We are releasing the UMA code, weights, and associated data to accelerate computational workflows and enable the community to build increasingly capable AI models.

1 Introduction

Density Functional Theory (DFT) models the interaction of atoms from first principles through the estimation of their electronic structure. It serves as the foundation of modern computational chemistry and materials science, and has provided insights into many applications including drug discovery [70, 78], energy storage [73, 27, 72], and semiconductors [62, 76]. Despite DFT’s widespread adoption, its considerable computational expense limits its usage.

Machine learning models offer the potential to accurately approximate DFT while being dramatically faster ($O(n)$ vs. $O(n^3)$ for DFT, where n is the number of atoms); reducing computation time from hours to less than a second. Ideally, these models – referred to as Machine Learning Interatomic Potentials (MLIPs) – would generalize across the many tasks that utilize DFT. We refer to a “task” as a chemical domain (e.g. materials, catalysts, molecules) plus the specialized DFT settings required by domain. For each task, we can explore different applications of DFT, such as molecular dynamics, relaxations, vibrational analysis, and mechanical response. Training MLIPs that generalize across such tasks remains an open problem.

*Co-first Author

\dagger Co-corresponding Author

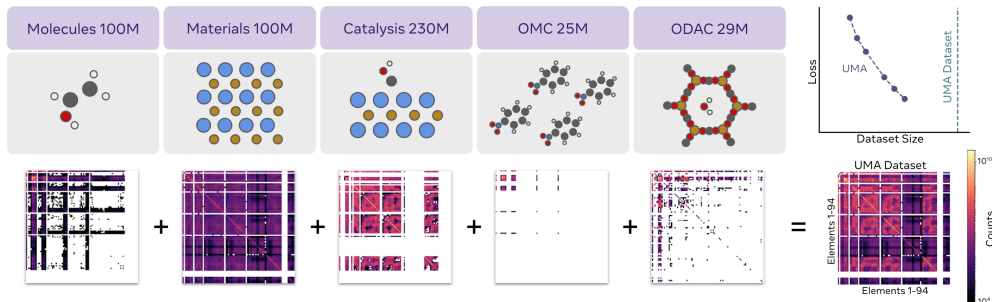


Figure 1: Visualization of the different datasets used for training. The 2D plots (bottom) illustrate the number of pairwise interactions contained in each dataset for every combination of elements. Note their combination covers nearly the entire chemical space with the exception of the radioactive elements. Model accuracies have improved with training dataset size (upper right), and this paper explores the limits of this scaling.

The scaling of datasets and model sizes has led to major breakthroughs in language and vision models, enabling their generalization across diverse data distributions and tasks [2, 24]. A similar scaling of atomic datasets is more challenging due to their computational cost, resulting in models typically being trained on smaller problem-specific datasets [57, 18, 17]. A potential solution is to pool data across tasks to allow for the creation of an exceptionally large dataset for training multi-task models. Recently, several large domain-specific datasets including catalysts [11, 72], materials [5, 67], and molecules [43] have been released that, when combined, total nearly half a billion atomic systems. This combined dataset defines a new paradigm in terms of the diversity of interactions and chemical environments (Figure 1), allowing for the learning of general-purpose models.

In this paper, we present a family of Universal Models for Atoms (UMA) designed to test the limits of accuracy, speed, and generalization for a single model across chemistry and materials science. The unprecedented amount of data ($\sim 500\text{M}$ atomic systems, Figure 1) poses new challenges in balancing accuracy and efficiency with multi-task training. To explore this space, we develop empirical scaling laws, relating compute, data, and model size, to determine the model size required to fit the UMA dataset and to define compute-optimal and inference-optimal training strategies. To accommodate the growing demand for model capacity while maintaining speed, we introduce a novel Mixture of Linear Experts (MoLE) architecture that efficiently scales the model size without increasing inference times for applications such as Molecular Dynamics (MD). For efficient model training, we propose a novel two-stage training schedule that efficiently pre-trains a model that is then refined in the second stage to conserve energy at higher precision.

We demonstrate that UMA, without fine-tuning to specific tasks, performs similarly or better in both accuracy and inference-speed/memory-efficiency than specialized models on a wide-range of material, molecular and catalysis benchmarks. Highlights include state-of-the-art results on the popular Matbench Discovery leaderboard [59], a 25% improvement in successful adsorption energy calculations for catalysis [42], and accuracy sufficient for practical applications (e.g. ligand-strain energy) in structure-based drug-design [43]. All code and data used for training UMA is publicly available. UMA model weights are available with a commercially permissive license (with some geographic and acceptable use restrictions).

2 Approach

An MLIP acts as a surrogate for DFT, and so it requires the same inputs as DFT: atom positions, their atomic numbers, and optionally spin and charge information. As outputs, MLIPs estimate the energy of an atomic structure from which other properties may be computed through the use of derivatives, such as per-atom forces, stress, etc. For many applications, such as molecular dynamics or performing relaxations, an MLIP is used to calculate the atomic forces to run simulations that can require thousands or even millions of iterations. For this reason, MLIPs must be both accurate and computationally efficient.

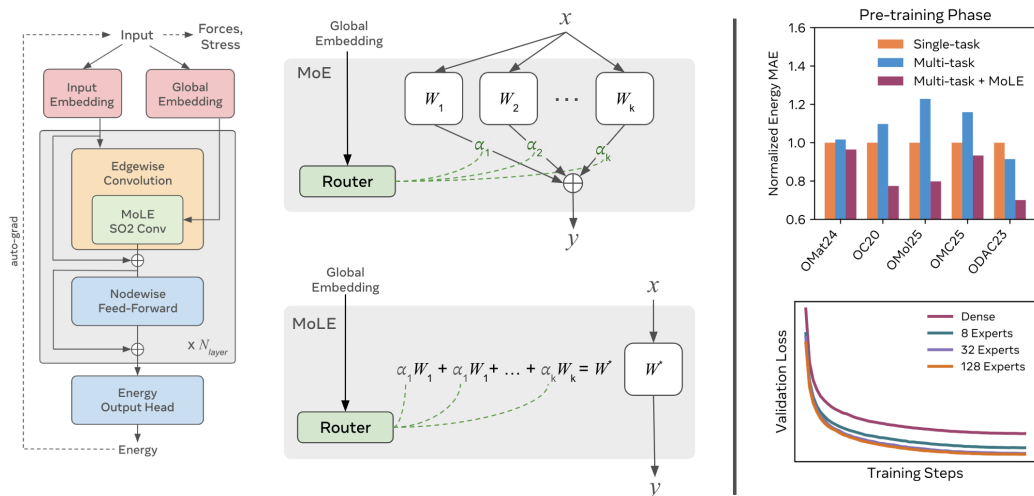


Figure 2: (left) Overview of UMA model architecture. The SO2 convolution is made up of a set of linear operations and each one of these operations is replaced with MoLE. (middle) Illustration of MoE and MoLE. The embedding used for routing, which estimates the expert weights α , only depends on global information making it possible to merge before the model forward pass (middle, bottom), which has substantial benefits for applications that require long roll outs such as molecular dynamics. (right) Bar plot of UMA-S trained with MoLE for multi-task and without MoLE for single and multi-task. Note the MoLE model outperforms non-MoLE models. (right, bottom) Loss plots when varying the number of experts from 1 to 128 for UMA-S.

Table 1: Summary of UMA models.

Model	Total Parameters	Active Parameters	Inferences per second for 1k Atoms	Max Atoms per 80GB GPU	Conservative
UMA-S	150M	6M	16	100k+	✓
UMA-M	1.4B	50M	3	10k+	✓
UMA-L	700M	700M	1.6	1k+	✗

Inference speed and max atoms measured on Nvidia H100 with a periodic system that has ≈ 50 neighbors per atom within 6\AA , see Appendix D

2.1 UMA: Universal Model for Atoms

In this paper, we describe a family of models that can be categorized into three sizes: small (S), medium (M), and large (L). A summary of the models can be found in Table 1. Additional details on the different versions of UMA can be found in Appendix E.1. All the models have different accuracy and speed attributes and as a result are best suited for distinct use cases. UMA-S aims to strike a balance between accuracy and efficiency and is suitable for computationally intensive applications such as long molecular dynamics simulations. The most general-purpose model of the family is UMA-M, which is more accurate and can be used as a DFT surrogate for relaxations or vibrational analysis as well as for molecular dynamics. UMA-L is a highly accurate DFT surrogate and is intended as a proof-of-principle to help understand scaling behavior and to demonstrate the limits of what is currently feasible.

We begin by providing a basic introduction to the UMA architecture. Next, we highlight our use of Mixture of Linear Experts (MoLE), an efficient way to scale capacity and add flexibility for training models across different DFT datasets and tasks. Lastly, we present an overview of the training procedure used for UMA models.

2.2 Architecture

The UMA architecture is based on eSEN [21], an equivariant graph neural network, with a number of important modifications to enable the model to efficiently scale and handle additional inputs, such as total charge and spin, and the DFT settings desired for emulation. The standard eSEN architecture

takes 3D atomic positions and atomic numbers as inputs and returns the total energy, per-atom forces, and, optionally, stress. The network operates by updating a spherical harmonic node embedding for each atom through a series of message passing layers. The embeddings are initialized based on the atom’s atomic number. Messages are passed between neighboring atoms that are less than a predefined distance (6 Å) from each other. Each message passing layer consists of an edge-wise block followed by a node-wise feed-forward block with residual connections. Normalization is performed after each layer. The central component of the edgewise block is the eSCN convolution [54]. After message passing, there is a single task-independent node-wise feed-forward block to predict the outputs.

2.2.1 Charge, Spin, and DFT Task Inputs

In addition to the inputs handled by eSEN, we expand the model to incorporate information about the system’s total charge, total spin multiplicity, and the DFT task. The charge and spin are indicated using an integer value for each and allow the MLIP to model structures which may be electrically charged (have extra or missing electrons) or have unpaired electrons. The DFT task indicates which of the five training dataset DFT settings the model should attempt to replicate. A single dataset is specified and a random vector corresponding to it is fed into the network. This is necessary since different datasets use different plane-wave or localized orbital DFT calculators (VASP [39, 38] and ORCA [50]) and levels of theory.

We introduce a new embedding to UMA models that enables the inclusion of charge, spin, and DFT task. Each of these inputs generates an embedding with the same dimension as the number of spherical channels used, which is concatenated and then fed through a 1-layer feed-forward network. The result is added to the node embeddings at each layer for the spherical harmonics coefficients of degree 0 ($L = 0$). This embedding is also used to compute the global embedding used for MoLE routing, which is described below.

2.3 Mixture of Linear Experts

A common approach to learning general-purpose models is to increase the amount and diversity of their training data. As datasets increase in size, scaling laws suggest model sizes must also be scaled to optimally reduce losses [24, 2]. However, this presents a tradeoff, which may lead to accurate models that are too computationally expensive to use in practical applications. One method to improve these trade-offs is to use Mixture of Experts [32, 31, 47] (MoEs) to increase the number of model parameters while minimizing the additional computational cost. In an MoE model, the outputs of a block are calculated by a set of experts, each with their own individual set of weights. Typically, a sparse weighted combination of their outputs is combined and passed to the next block. This approach has been shown to work well for LLMs to improve both their efficiency and their ability to generalize [19, 33, 60, 15].

The application of MoEs to MLIPs requires additional considerations. Contrary to language modeling, estimating the potential energy surface is a regression task whose outputs should vary smoothly to ensure energy conservation [21]. In addition, the estimated forces should be equivariant to rotation. This implies that the use of experts should not introduce discontinuities on the energy surface, and care must be taken to ensure equivariance is maintained. Another practical consideration for MLIPs is that the task and set of atoms is commonly held constant during long simulations. Ideally, an MoE approach for MLIPs would take advantage of this to improve efficiency in sequential inference applications.

We propose using a Mixture of Linear Experts (MoLE) for MLIPs. An MoLE combines a set of linear experts [46, 31]:

$$y = \sum_k \alpha_k (W_k x) \tag{1}$$

where each expert k has a set of weights W_k and contribution $\alpha_k \in [0, 1]$. While this was one of the original approaches proposed for MoEs [31], MoEs that use sparse sets of non-linear experts which compete for attention [32] are much more commonly used in modern networks [19, 60, 15, 63]. However, MoLEs offer distinct advantages for MLIPs. First, the MLIP can learn functions that share information and vary smoothly between tasks by encouraging the dense use of all experts without enforcing sparseness. Second, since MoLE is a mixture of linear experts, they maintain

rotational equivariance when used within the eSCN convolution [54]. Finally, if the expert weights are only dependent on time-invariant global information such as element composition, the network weights may be precomputed before running simulations [46, 75]. The precomputed weights W^* are calculated by moving the summation in Equation 1, which results in MoE inference times that are similar to non-MoE models:

$$y = W^*x \quad \text{where} \quad W^* = \left(\sum_k \alpha_k W_k \right) \quad (2)$$

The contribution α_k of each expert is calculated as a function of system-level features, including element composition, charge, spin, and task information. Embeddings are calculated for each of these properties, concatenated, and passed through a 3-layer MLP followed by a softmax to estimate α_k , $\sum_k \alpha_k = 1$. We specifically exclude information when calculating α 's that may vary during the course of relaxations or MD simulations, such as relative atom positions or other neighborhood information.

2.4 Training Procedure

Training models on large datasets across numerous tasks is challenging due to the computational resources required. This is especially true for conservative models, which require an additional backward pass to calculate forces or stress. To improve training efficiency, we implemented a two-stage approach described in detail in the supplementary material (Appendix A). As proposed by [21, 7], we train a model that directly predicts forces in the first stage. In the second stage, we remove the force head and fine-tune the model to predict conserving forces and stresses using auto-grad. This approach takes advantage of the faster training enabled by direct models, while providing energy conservation and smooth potential energy landscapes required by many applications.

Several other novel improvements were made to each stage’s training to further improve efficiency. Half-precision is critical to training efficiently on modern GPUs. Similar to other domains such as LLM training, we found that BF16 is significantly more stable compared to FP16 with automatic mixed precision. However, unlike LLMs, MLIPs are significantly more sensitive to numerical precision; we observed that BF16 alone will degrade accuracy by as much as 20 – 50% depending on the task and the property being computed. We found that pre-training with BF16 and switching to FP32 for fine-tuning recovers the loss in accuracy. Finally, training the models with a large number of MoLE experts is challenging due to memory constraints. We make further optimization to help bound and amortize memory usage (Appendix A). In addition, models were trained with a combination of graph parallelism [66] and fully-sharded data parallelism for large MoLE layers and activation checkpointing (Appendix A). When combined, this allows us to reliably scale up model training up to 10B total parameters.

The energies for each dataset can vary significantly due to the use of different DFT settings, which makes multi-task training difficult. To account for this, an energy referencing scheme was employed as described in Appendix A.6. This approach allowed for the use of a single energy head across all tasks without the need for task-specific heads.

3 Datasets

To train a model capable of generalizing across DFT tasks, an ideal training dataset would include materials, molecules, and their interactions. The Open Molecules 2025 (OMol25) [43] and Open Materials 2024 (OMat24) [5] datasets cover both molecules and materials respectively. The Open Catalyst 2020 (OC20) [11] and OpenDAC 2025 (ODAC25) [68] datasets are useful for modeling the interactions of molecules and materials. Finally, the Open Molecular Crystals 2025 (OMC25) [23] dataset specializes in modeling the interaction between molecules in periodic structures. In combination, these datasets contain close to 500 million training examples with over 30 billion atoms. As visualized in Figure 1, the combination of these datasets contains nearly all pairwise interactions between atoms of different elements. We focused on large datasets, because of the challenges of mixing different DFT tasks and since the inclusion of much smaller datasets was unlikely to significantly impact the model weights.

While all DFT calculations yield energy and force labels by determining ground-state electronic structures, different chemical systems require domain-specific DFT settings. For instance, the OMat24

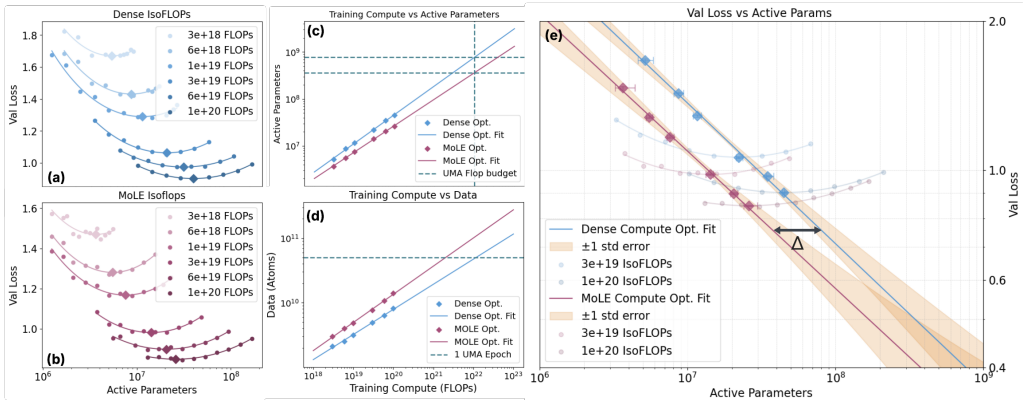


Figure 3: Empirical scaling measurements of dense (blue) vs. MoLE (red) model architectures. FLOPs vs. validation loss for (a) dense and (b) MoLE (8-expert) models. Experiment sets are performed by holding FLOPs constant and varying model size and training data. Diamonds represent the compute optimal frontier. (c) Training compute vs. parameters. Vertical green dotted line represents our estimated training budget of $O(10^{22})$ FLOPs, horizontal dotted lines are corresponding dense and MoLE model sizes. (d) Compute vs. dataset size (atoms) with the green dotted line representing the training FLOPs required for 1 epoch of UMA training data (50B atoms) (e) Overlay of dense vs. MoLE compute optimal frontiers from (a-b) and the fitted power law of validation loss as a function of parameters. A compute optimal MoLE model with $\Delta \approx 2.5 \times$ fewer active parameters can achieve an equivalent loss. Fitting details and parameters are described in Appendix C.

dataset uses the PBE functional and is generated with the plane-wave code VASP, whereas OMol25 employs the ω B97M-V functional with the localized orbital code ORCA. Designing a single model that performs well across such diverse settings is a non-trivial challenge. Additionally, the datasets differ in size and information content, so we adjust their sampling ratios: 4 for OMat24 and OMol25, 1 for OC20 and ODAC25, and 2 for OMC25. Further details on the datasets and our unified modeling strategy can be found in Appendix B and A respectively.

4 Results

4.1 Model and Data Scaling

In various domains such as language, empirical power-law relationships have been successfully used [28, 24, 35] to predict the optimal model size and quantity of training data given a fixed compute budget. However, for modeling MLIPs, no models have been trained on the size of UMA’s dataset and very few models have been trained to $>100M$ parameters [5]; we do not know whether such relationships exist or whether the models will continue to improve with data and parameters. In this study, we show that UMA models do show log-linear scaling behavior as seen in other domains in the FLOP ranges we tested, indicating that greater model capacity is required to fit the UMA dataset. We used these scaling relationships to select the appropriate model size for our dataset and demonstrate the advantage of MoLE over the dense architecture.

Following [28, 24, 35], we first examine the behavior of training compute in FLOPs C as a function of model size N and dataset size D . To determine this, we used total validation loss (computed in the same way as training loss) as the observable quantity. We trained a series of models by sweeping the model parameter size while fixing the training compute budget in FLOPs. This is done by varying the amount of training data for each model, i.e., smaller models receive more training data, while larger models receive less. This is performed for both the dense and MoLE (8 expert) models classes, producing "Iso-FLOPs" curves Figure 3(a,b). The minima of the Iso-FLOPs represent the compute optimal model, or the best achievable loss for the given compute budget (diamonds in Figure 3).

Optimal model size. We fit the Iso-FLOPs minima using power laws [35, 28] to estimate the optimal model and dataset sizes given a fixed compute budget (detailed in Appendix C). Figure 3(c,d)

indicates that the dense and MoLE models display convincing log-linear scaling behavior at the scales of our experiments ($10^{18} - 10^{20}$ FLOPs). Given that our training dataset was approximately 50 billion atoms (1 epoch) and our estimated compute budget for pretraining was $O(10^{22})$ FLOPs (extrapolated from our preliminary training runs), Figure 3(c) suggests the largest compute optimal dense model we should train is $\sim 700\text{M}$ parameters corresponding to the UMA-L. In practice, we used the compute optimal model size as a starting point and continued training beyond the compute optimal regime to produce lower losses while minimizing parameter sizes. However, we observed that training on too many epochs can lead to overfitting and significantly deviate from log-linear scaling behavior, prompting us to keep our training within 2-3 epochs.

Dense vs MoLE. If we combine Figures 3(a,b) and fit the Iso-FLOPs minima as a function of loss (Figure 3(e)), we can compare the model sizes needed by the dense and MoLE models to achieve a fixed loss. Effectively, an optimal MoLE model can achieve the same loss as an optimal dense model that is Δ times larger, e.g., $\Delta \approx 2.5 \pm 0.2$ for UMA-M. We observe that this advantage is reduced at larger model sizes; training a 700M active parameter (8 expert - 5.6B parameter total) MoLE model had marginal improvement over the dense version. This effect can be seen in overlaid IsoFLOPs in Figure 3(e). As parameters increase, dense and MoLE performance converge. We hypothesize that we are limited by our dataset’s size, regardless of MoLE or dense architectures.

4.2 Multi-task vs. Single-Task

To explore the benefits of MoLE models for multi-task training, we compare UMA-S (with MoLE) to non-MoLE dense models trained for single/multi-task in Figure 2 (right, top). In this limited parameter regime, multi-task models trained without MoLE always perform worse than single-task (ST) models. With the use of MoLE, UMA-S can achieve results comparable to task specialized small models. We also experimented with varying the number of experts for UMA-S in Figure 2 (right, bottom). A significant improvement in loss is observed when moving from 1 expert to 8. A smaller gain is found with 32 experts, and the additional gain from 32 to 128 experts is negligible. In our experiments, UMA-S uses 32 experts. For large models, multi-task training offers benefits even without MoLE, as shown in Appendix F, where multi-task models avoid overfitting and generally achieve better performance.

4.3 Inference Efficiency

The ability to increase the length scale (number of atoms) and time scale of molecular dynamics (MD), relaxations and other types of long running simulations is critical to our design. Leveraging our MoLE strategy, we can pre-merge all the weights and pay no additional penalty in inference time or memory when running a long time-scale simulations on a single system. Here we show that UMA models, despite having very large parameter counts and achieving SOTA accuracy across many domains, are extremely competitive in simulation settings in both speed and raw number of atoms that can fit in memory compared to specialized single-domain models. For example, the UMA-S can simulate 1000 atoms at 16 steps per second (1.4 ns-per-day) and fit system sizes up 100,000 or more atoms in memory on a single 80GB GPU. Lastly, our models are designed to be scaled with multi-GPU parallel inference using the Graph Parallelism strategy [66] described in training; giving the potential to provide orders of magnitude speed-ups when running simulations at the 100k+ atoms scale and unlock new science that is not possible today. We will leave multi-GPU inference outside the scope of this paper.

4.4 Evaluation

Our evaluation contains two main components: (1) a diverse set of held-out test splits (Table 2) and (2) a suite of practically important benchmarks (Table 3). To cover all chemical domains studied: materials, catalysis, molecules, molecular crystals, and metal-organic frameworks (MOFs), we propose new test sets and benchmarks, in addition to established benchmarks in existing literature. We highlight selected results below, with a more detailed discussion in Appendix E.

Materials. In Table 2, we report the test-set performance on two OOD test sets: WBM [74] and high entropy alloy (HEA). The HEA test set is introduced in this work (Appendix E.2). UMA-M performs on-par with SOTA task specialized models, such as eSEN-30M-OMat and eqV2-OMat. The degraded performance of UMA-L on energy of the HEA dataset (Table 11) suggests overfitting,

Table 2: Test MAE results on held out test splits for materials [59], catalysis [11], molecules [43], molecular crystals [23] and MOFs [67]. All energies are in meV, forces are in meV/Å and stresses are in meV/Å³. Results for UMA are compared against the SOTA literature results. Target accuracies for practical utility are provided as an approximate guide for reference.

Model	Materials						Catalysis				Molecules				Molecular crystals			MOFs	
	WBM Energy/Atom	Forces	Stress	HEA Energy/Atom	Forces	Stress	ID Ads. Energy	Forces	OOD-Both Ads. Energy	Forces	OOD-Comp Energy/Atom	Forces	PDB-TM Energy/Atom	Forces	OMC-Test Energy/Atom	Forces	Stress	OOD-LT Ads. Energy	Forces
UMA																			
UMA-S-1.1	20.2	62.8	4.4	24.9	83.7	3.5	51.5	24.1	68.8	30.7	0.95	8.64	0.84	15.47	1.03	5.04	0.93	289.9	13.3
UMA-M-1.1	18.2	50.7	4.2	21.9	69.0	3.5	31.8	15.5	45.5	20.2	0.74	5.44	0.50	10.14	0.84	2.83	0.90	294.1	10.3
Literature																			
eSEN-30M-OAM [21]	16.2	49.6	4.1	20.0	59.5	3.2	-	-	-	-	-	-	-	-	-	-	-	-	-
eqV2-OAM [5]	14.9	46.3	3.6	20.3	47.0	2.7	-	-	-	-	-	-	-	-	-	-	-	-	-
eqV2-OC20 [44]	-	-	-	-	-	-	149.1	11.6	306.5	15.7	-	-	-	-	-	-	-	-	-
GemNet-OC20 [22]	-	-	-	-	-	-	163.5	16.3	343.3	23.1	-	-	-	-	-	-	-	-	-
eqv2-ODAC [67]	-	-	-	-	-	-	-	-	-	-	-	-	-	-	-	-	-	316.0	7.2
eSEN-sm-cons. [43]	-	-	-	-	-	-	-	-	-	-	1.35	7.39	0.83	12.72	-	-	-	-	-
eSEN-S-OMC [23]	-	-	-	-	-	-	-	-	-	-	-	-	-	1.05	5.39	0.94	-	-	-
Target																			
Practical Utility	10-20	-	-	10-20	-	-	100	-	100	-	1-3	-	1-3	-	1-3	-	-	100	-

Table 3: Evaluation results on Matbench-Discovery [59], MDR phonon [45], elastic tensor [16, 34], and AdsorbML benchmarks [42]. Results are also provided for a diverse set of molecule [43] and molecular crystal [29, 23] benchmarks. NVE MD [21] tests whether energy conservation is observed when running the model for molecular dynamics. SOTA results from literature are reported where available. Additionally, for the materials evaluations, UMA models were fine-tuned on MPTrj [17] and sAlex [61, 5] to be consistent with the benchmark’s DFT settings.

Model	Materials								Catalysis	Molecules				Molecular Crystals				
	Matbench [59] F1	RMSD	MAE [eV/atom]	κ_{SRME} [56]	Phonons [45] ω_{max} [K]	Free Energy [kJ/mol]	Elasticity [16, 34] C_{ym} [GPa]	K_{sh} [GPa]	NVE MD [21] Conserve	AdsorbML [42] Success Rate	OMoL25 [43] Ligand-strain [meV]	PDB-pocket [meV]	Dist-SR [meV]	Dist-LR [meV]	NVE MD [21] Conserve	CSP Targets [29] Lattice Energy [kJ/mol]	Kendall Rank	RMSD [Å]
UMA																		
UMA-S-1.1	0.913	0.064	0.020	0.204	18.82	5.48	9.47	5.16	✓	66.80%	4.86	127.7	20.4	194.7	✓	2.13	0.86	0.13
UMA-M-1.1	0.929	0.061	0.018	0.176	14.81	3.87	8.57	4.78	✓	72.25%	2.96	76.8	15.5	138.1	✓	3.24	0.82	0.14
Literature																		
eSEN-30M-OAM [21]	0.925	0.061	0.018	0.170	15.00	4.00	9.13	5.73	✓	-	-	-	-	-	-	-	-	-
ORB v3 [58]	0.905	0.075	0.024	0.210	-	-	-	-	-	-	-	-	-	-	-	-	-	-
SevenNet-MF-ompa [36]	0.901	0.064	0.021	0.317	-	-	-	-	-	-	-	-	-	-	-	-	-	-
GRACE-2L-OAM [8]	0.880	0.067	0.023	0.294	-	-	-	-	-	-	-	-	-	-	-	-	-	-
MACE-MPA-0 [6]	0.852	0.073	0.028	0.412	-	-	-	-	-	-	-	-	-	-	-	-	-	-
eqv2-OC20 [42]	-	-	-	-	-	-	-	-	-	60.80%	-	-	-	-	-	-	-	-
GemNet-OC20 [42]	-	-	-	-	-	-	-	-	-	54.88%	-	-	-	-	-	-	-	-
eSEN-sm-cons. [43]	-	-	-	-	-	-	-	-	-	-	4.66	147.3	21.6	197.0	✓	-	-	-
eSEN-S-OMC [23]	-	-	-	-	-	-	-	-	-	-	-	-	-	-	6.18	0.74	0.18	

and demonstrates the test set’s challenging nature. In Table 3, we report benchmark results on the prediction of materials’ thermodynamic stability, thermal conductivity, and vibrational properties. Note for these results, the UMA models are fine-tuned on the MPTrj [17] and sAlex [61, 5] to be consistent with the DFT settings of the public benchmarks. On the popular benchmark Matbench-Discovery (MBD) [59], UMA-M achieves the highest F1 score to date. All UMA models of different sizes show strong performance, which suggests that further scaling of model sizes is unlikely to result in better performance on the MBD benchmark. The conserving UMA models (S and M) also excel at phonon-related properties, which are reflected by metrics including κ_{SRME} , free energy MAE, and shear/bulk elasticity MAE.

Catalysis. We evaluate our models on two established catalysis benchmarks: OC20 S2EF [11] and AdsorbML [42]. These benchmarks focus on adsorption energy predictions – that is, the models predict the change in energy as a molecule, known as an adsorbate, comes in contact with a surface. Most previous models on the OC20 benchmark directly predict the adsorption energy given the adsorbate’s position on the surface. Since our model predicts total energy, we make a total energy prediction on the same structure, and another on a clean surface without the adsorbate [1]. These two values are subtracted (along with the energy of the adsorbate in isolation) to predict the adsorption energy. As shown in Table 2, UMA models significantly outperform previous SOTA models on OC20 S2EF adsorption energy prediction – reducing the errors by around 80%. On the more realistic

benchmark of AdsorbML, which evaluates a model’s capability to predict the global minimum adsorption energy, all UMA models outperform the previous SOTA (EquiformerV2). In particular, UMA-L achieves a 25% improvement in the success rate (Table 12).

Molecules. Initial UMA models were trained on a preview subset ($\approx 70\%$) of the OMol25 dataset, since portions of the dataset were still being calculated when UMA model training began (results in Appendix E). Both UMA-1 and UMA-1.1 were trained on the full OMol25 dataset. In Table 2, we report the prediction performance on two challenging test splits of OMol25: OOD-Comp and OOD PDB-TM. Our results show that UMA-S achieves performance comparable to the domain-specific eSEN-sm-cons, while UMA-M significantly outperforms both models. In Table 3, we evaluate ligand strain and pocket–ligand interaction energy, which are quantities relevant to structure-based drug discovery. In particular, for ligand strain (and, similarly, for conformers in Table 19), UMA-M achieves errors approaching those of the DFT reference, demonstrating its ability to act as a practical surrogate for these calculations. On the distance scaling benchmarks (short and long range) in Table 3, UMA-S slightly surpasses eSEN-sm-cons despite having the same receptive field.

Molecular Crystals. In contrast to materials, molecules, and catalysis, the development and use of universal MLIPs for molecular crystals has been relatively underexplored. In addition to the OMC25 test set, we evaluate our UMA’s capability to accurately predict lattice energies, rank, and match structures of the most recent 7th Crystal Structure Prediction (CSP) Blind Test [29]. In all evaluations, UMA-S outperforms the task-specific eSEN-S-OMC baseline, which was trained on the OMC25 dataset [23]. The high accuracy of lattice energy predictions (≤ 3 kJ/mol) indicates that UMA can be a reliable substitute for DFT in many crystal structure prediction applications.

Metal Organic Frameworks. Computing the adsorption energy of CO₂ for a MOF sorbent is important for direct-air carbon capture applications and an established benchmark [67]. Similar to OC20, UMA models use total energy predictions to compute the adsorption energy. UMA models perform on par with previous SOTA models on the ID test set (Appendix E) while achieving the best performance on the hardest ODAC OOD test set (Table 2), suggesting improved generalization.

5 Related Work

5.1 Universal MLIPs

The field of MLIPs has been rapidly improving due in part to the availability of larger datasets. A recent example in the materials space is the release of the Alexandria [61] and OMat24 [5] datasets, which quickly led to improved performance on the Matbench-Discovery leaderboard [59]. While MLIPs trained on these materials datasets are often referred to as "universal" because they include nearly all the elements in the periodic table [12, 6, 20, 51, 48, 77, 53], they may not generalize well to other domains such as molecules [37] or surfaces [11]. One reason for this is the chemical, structural, and elemental distribution shifts between materials and other domains such as molecules. Another reason is the level of DFT theory that is considered accurate differs between domains, e.g. PBE for materials and ω B97M-V for molecules. As we demonstrate, training across domains can lead to unified representations and help generalization.

While there have been a number of promising works exploring training MLIPs across multiple domains, it remains an open challenge to demonstrate high-accuracy zero-shot performance. One approach is to pre-train a model using a large corpus of data (> 100 M) and fine-tuning for specific tasks [65, 79]. The fine-tuned models are shown to perform significantly better than models trained from scratch. Nevertheless, removing the need for specialization would make these models substantially more useful. Recent studies suggest that achieving zero-shot performance across two DFT tasks may be possible [36, 64].

5.2 Scaling Relations

Empirical scaling laws provide a wealth of insight into the relationships between compute, data, and model size. In LLMs, scaling laws motivated the community to train on more tokens with larger models because performance improvements became predictable [28, 24, 35]. Additionally, scaling relations help practitioners decide on how to best (compute-optimal) allocate resources such as dataset and model size. These types of relations have been explored in MLIPs to compare the asymptotic

scaling behavior of different model architectures and training paradigms. For example, [10] showed that equivariant models have different scaling behavior compared to non-equivariant models.

6 Limitations

While UMA represents a significant step forward, there are still limitations and areas for improvement. Currently, the UMA models are limited in their ability to model long-range interactions. Our small and medium models use a standard MLIP cutoff distance of 6Å, the actual receptive field is much larger due to message passing, but this can present a problem for inputs where sets of atoms are separated by more than 6Å. For example, if an adsorbate starts at 7Å from a catalyst’s surface the model views these as two independent non-interacting structures. Improvements may also be made in how charge and spin are incorporated into the model [17]. Currently, each discrete charge or spin uses a separate embedding, which limits its ability to generalize to unseen spins or charges.

Our work aims to accelerate scientific discovery in chemistry and materials science using MLIPs; however, potential misuses exist, and we train on datasets designed for applications beneficial to society to mitigate these risks.

7 Discussion and Conclusion

We explore techniques for training MLIPs across diverse DFT tasks using nearly 500 million training examples gathered over numerous datasets. By taking advantage of scaling relationships between dataset size, model capacity and loss, we are able to train models that are competitive with—or better than—task specialized models. Naive approaches to scaling model parameters would result in an accurate but slow model. To address this, we introduced Mixture of Linear Experts, a method to increase model capacity while maintaining inference efficiency. Among our family of models, UMA-S offers a favorable balance between speed and accuracy, capable of performing MD simulations of 1,000 atoms at 1.4ns per day on a single 80GB GPU.

We evaluated UMA across a wide-range of benchmarks for materials, molecules, catalysts, molecular crystals, and metal organic frameworks, demonstrating strong performance across all. For well established benchmarks, such as AdsorbML and Matbench Discovery, we achieve new state-of-the-art results. Looking ahead, the development of more challenging benchmarks will be crucial for driving progress in the field.

Our findings suggest that a single model can achieve sufficient accuracy for practical research applications across a broad spectrum of chemistry and materials science applications. This paves the way for universal MLIPs and opens new opportunities for atomic simulations at scale.

References

- [1] Kareem Abdelmaqsood, Muhammed Shuaibi, Adeesh Kolluru, Raffaele Cheula, and John R. Kitchin. Investigating the error imbalance of large-scale machine learning potentials in catalysis. *Catal. Sci. Technol.*, 14:5899–5908, 2024. doi: 10.1039/D4CY00615A.
- [2] Josh Achiam, Steven Adler, Sandhini Agarwal, Lama Ahmad, Ilge Akkaya, Florencia Leoni Aleman, Diogo Almeida, Janko Altenschmidt, Sam Altman, Shyamal Anadkat, et al. Gpt-4 technical report. *arXiv preprint arXiv:2303.08774*, 2023.
- [3] Qianxiang Ai, Vinayak Bhat, Sean M. Ryno, Karol Jarolimek, Parker Sornberger, Andrew Smith, Michael M. Haley, John E. Anthony, and Chad Risko. OCELOT: An infrastructure for data-driven research to discover and design crystalline organic semiconductors. *The Journal of Chemical Physics*, 154(17):174705, May 2021. ISSN 0021-9606. doi: 10.1063/5.0048714.
- [4] Luis Barroso-Luque, Julia H. Yang, Fengyu Xie, Tina Chen, Ronald L. Kam, Zinab Jadidi, Peichen Zhong, and Gerbrand Ceder. SMOL: A Python package for cluster expansions and beyond. *Journal of Open Source Software*, 7(77):4504, 2022. ISSN 2475-9066. doi: 10.21105/joss.04504.

- [5] Luis Barroso-Luque, Muhammed Shuaibi, Xiang Fu, Brandon M Wood, Misko Dzamba, Meng Gao, Ammar Rizvi, C Lawrence Zitnick, and Zachary W Ulissi. Open materials 2024 (omat24) inorganic materials dataset and models. *arXiv preprint arXiv:2410.12771*, 2024.
- [6] Ilyes Batatia, Philipp Benner, Yuan Chiang, Alin M Elena, Dávid P Kovács, Janosh Riebesell, Xavier R Advincula, Mark Asta, Matthew Avaylon, William J Baldwin, et al. A foundation model for atomistic materials chemistry. *arXiv preprint arXiv:2401.00096*, 2023.
- [7] Filippo Bigi, Marcel Langer, and Michele Ceriotti. The dark side of the forces: assessing non-conservative force models for atomistic machine learning. *arXiv preprint arXiv:2412.11569*, 2024.
- [8] Anton Bochkarev, Yury Lysogorskiy, and Ralf Drautz. Graph atomic cluster expansion for semilocal interactions beyond equivariant message passing. *Physical Review X*, 14(2):021036, 2024.
- [9] Stanislav S. Borysov, R. Matthias Geilhufe, and Alexander V. Balatsky. Organic materials database: An open-access online database for data mining. *PLOS ONE*, 12(2):e0171501, February 2017. ISSN 1932-6203. doi: 10.1371/journal.pone.0171501.
- [10] Johann Brehmer, Sönke Behrends, Pim de Haan, and Taco Cohen. Does equivariance matter at scale? *arXiv preprint arXiv:2410.23179*, 2024.
- [11] Lowik Chanussot, Abhishek Das, Siddharth Goyal, Thibaut Lavril, Muhammed Shuaibi, Morgane Riviere, Kevin Tran, Javier Heras-Domingo, Caleb Ho, Weihua Hu, et al. Open catalyst 2020 (oc20) dataset and community challenges. *Acs Catalysis*, 11(10):6059–6072, 2021.
- [12] Chi Chen and Shyue Ping Ong. A universal graph deep learning interatomic potential for the periodic table. *Nature Computational Science*, 2(11):718–728, 2022.
- [13] Yongchul G. Chung, Jeffrey Camp, Maciej Haranczyk, Benjamin J. Sikora, Wojciech Bury, Vaiva Krungleviciute, Taner Yildirim, Omar K. Farha, David S. Sholl, and Randall Q. Snurr. Computation-ready, experimental metal–organic frameworks: A tool to enable high-throughput screening of nanoporous crystals. *Chem. Mater.*, 26(21):6185–6192, 2014. doi: 10.1021/cm502594j.
- [14] Yongchul G. Chung, Emmanuel Haldoupis, Benjamin J. Bucior, Maciej Haranczyk, Seulchan Lee, Hongda Zhang, Konstantinos D. Vogiatzis, Marija Milisavljevic, Sanliang Ling, Jeffrey S. Camp, Ben Slater, J. Ilja Siepmann, David S. Sholl, and Randall Q. Snurr. Advances, updates, and analytics for the computation-ready, experimental metal–organic framework database: Core mof 2019. *J. Chem. Eng. Data*, 64(12):5985–5998, 2019. doi: 10.1021/acs.jced.9b00835.
- [15] Damai Dai, Chengqi Deng, Chenggang Zhao, RX Xu, Huazuo Gao, Deli Chen, Jiashi Li, Wangding Zeng, Xingkai Yu, Yu Wu, et al. Deepseekmoe: Towards ultimate expert specialization in mixture-of-experts language models. *arXiv preprint arXiv:2401.06066*, 2024.
- [16] Maarten de Jong, Wei Chen, Thomas Angsten, Anubhav Jain, Randy Notestine, Anthony Gamst, Marcel Sluiter, Chaitanya Krishna Ande, Sybrand van der Zwaag, Jose J. Plata, Cormac Toher, Stefano Curtarolo, Gerbrand Ceder, Kristin A. Persson, and Mark Asta. Charting the complete elastic properties of inorganic crystalline compounds. *Scientific Data*, 2(1):150009, March 2015. ISSN 2052-4463. doi: 10.1038/sdata.2015.9.
- [17] Bowen Deng, Peichen Zhong, KyuJung Jun, Janosh Riebesell, Kevin Han, Christopher J Bartel, and Gerbrand Ceder. Chgnet as a pretrained universal neural network potential for charge-informed atomistic modelling. *Nature Machine Intelligence*, 5(9):1031–1041, 2023.
- [18] Peter Eastman, Pavan Kumar Behara, David L Dotson, Raimondas Galvelis, John E Herr, Josh T Horton, Yuezhi Mao, John D Chodera, Benjamin P Pritchard, Yuanqing Wang, et al. Spice, a dataset of drug-like molecules and peptides for training machine learning potentials. *Scientific Data*, 10(1):11, 2023.
- [19] William Fedus, Barret Zoph, and Noam Shazeer. Switch transformers: Scaling to trillion parameter models with simple and efficient sparsity. *Journal of Machine Learning Research*, 23(120):1–39, 2022.

- [20] Bruno Focassio, Luis Paulo M. Freitas, and Gabriel R Schleder. Performance assessment of universal machine learning interatomic potentials: Challenges and directions for materials' surfaces. *ACS Applied Materials & Interfaces*, 2024.
- [21] Xiang Fu, Brandon M Wood, Luis Barroso-Luque, Daniel S Levine, Meng Gao, Misko Dzamba, and C Lawrence Zitnick. Learning smooth and expressive interatomic potentials for physical property prediction. *arXiv preprint arXiv:2502.12147*, 2025.
- [22] Johannes Gasteiger, Muhammed Shuaibi, Anuroop Sriram, Stephan Günnemann, Zachary Ulissi, C Lawrence Zitnick, and Abhishek Das. Gemnet-oc: developing graph neural networks for large and diverse molecular simulation datasets. *arXiv preprint arXiv:2204.02782*, 2022.
- [23] Vahe Gharakhanyan, Luis Barroso-Luque, Yi Yang, Muhammed Shuaibi, Kyle Michel, Daniel S. Levine, Misko Dzamba, Xiang Fu, Meng Gao, Xingyu Liu, Haoran Ni, Keian Noori, Brandon M. Wood, Matt Uyttendaele, Arman Boromand, C. Lawrence Zitnick, Noa Marom, Zachary W. Ulissi, and Anuroop Sriram. Open molecular crystals 2025 (omc25) dataset and models, 2025. URL <https://arxiv.org/abs/2508.02651>.
- [24] Aaron Grattafiori, Abhimanyu Dubey, Abhinav Jauhri, Abhinav Pandey, Abhishek Kadian, Ahmad Al-Dahle, Aiesha Letman, Akhil Mathur, Alan Schelten, Alex Vaughan, et al. The llama 3 herd of models. *arXiv preprint arXiv:2407.21783*, 2024.
- [25] Stefan Grimme, Jens Antony, Stephan Ehrlich, and Helge Krieg. A consistent and accurate ab initio parametrization of density functional dispersion correction (DFT-D) for the 94 elements H-Pu. *The Journal of Chemical Physics*, 132(15):154104, April 2010. ISSN 0021-9606. doi: 10.1063/1.3382344.
- [26] Bjørk Hammer, Lars Bruno Hansen, and Jens Kehlet Nørskov. Improved adsorption energetics within density-functional theory using revised perdew-burke-ernzerhof functionals. *Physical Review B*, 59(11):7413, 1999.
- [27] Qiu He, Bin Yu, Zhaohuai Li, and Yan Zhao. Density functional theory for battery materials. *Energy & Environmental Materials*, 2(4):264–279, 2019.
- [28] Jordan Hoffmann, Sebastian Borgeaud, Arthur Mensch, Elena Buchatskaya, Trevor Cai, Eliza Rutherford, Diego de Las Casas, Lisa Anne Hendricks, Johannes Welbl, Aidan Clark, et al. Training compute-optimal large language models. *arXiv preprint arXiv:2203.15556*, 2022.
- [29] Lily M Hunnisett, Nicholas Francia, Jonas Nyman, Nathan S Abraham, Srinivasulu Aitipamula, Tamador Alkhidir, Mubarak Almehairbi, Andrea Anelli, Dylan M Anstine, John E Anthony, et al. The seventh blind test of crystal structure prediction: Structure ranking methods. *Acta Crystallographica Section B: Structural Science, Crystal Engineering and Materials*, 80(6): 548–574, December 2024. ISSN 2052-5206. doi: 10.1107/S2052520624008679.
- [30] Lily M Hunnisett, Jonas Nyman, Nicholas Francia, Nathan S Abraham, Claire S Adjiman, Srinivasulu Aitipamula, Tamador Alkhidir, Mubarak Almehairbi, Andrea Anelli, Dylan M Anstine, et al. The seventh blind test of crystal structure prediction: Structure generation methods. *Acta Crystallographica Section B: Structural Science, Crystal Engineering and Materials*, 80(6): 517–547, December 2024. ISSN 2052-5206. doi: 10.1107/S2052520624007492.
- [31] Robert A Jacobs, Michael I Jordan, and Andrew G Barto. Task decomposition through competition in a modular connectionist architecture: The what and where vision tasks. *Cognitive science*, 15(2):219–250, 1991.
- [32] Robert A Jacobs, Michael I Jordan, Steven J Nowlan, and Geoffrey E Hinton. Adaptive mixtures of local experts. *Neural computation*, 3(1):79–87, 1991.
- [33] Albert Q Jiang, Alexandre Sablayrolles, Antoine Roux, Arthur Mensch, Blanche Savary, Chris Bamford, Devendra Singh Chaplot, Diego de las Casas, Emma Bou Hanna, Florian Bressand, et al. Mixtral of experts. *arXiv preprint arXiv:2401.04088*, 2024.
- [34] Aaron D. Kaplan, Runze Liu, Ji Qi, Tsz Wai Ko, Bowen Deng, Janosh Riebesell, Gerbrand Ceder, Kristin A. Persson, and Shyue Ping Ong. A Foundational Potential Energy Surface Dataset for Materials, March 2025.

- [35] Jared Kaplan, Sam McCandlish, Tom Henighan, Tom B Brown, Benjamin Chess, Rewon Child, Scott Gray, Alec Radford, Jeffrey Wu, and Dario Amodei. Scaling laws for neural language models. *arXiv preprint arXiv:2001.08361*, 2020.
- [36] Jaesun Kim, Jisu Kim, Jaehoon Kim, Jiho Lee, Yutack Park, Youngho Kang, and Seungwu Han. Data-efficient multifidelity training for high-fidelity machine learning interatomic potentials. *Journal of the American Chemical Society*, 147(1):1042–1054, 2024.
- [37] Dávid Péter Kovács, J Harry Moore, Nicholas J Browning, Ilyes Batatia, Joshua T Horton, Venkat Kapil, William C Witt, Ioan-Bogdan Magdău, Daniel J Cole, and Gábor Csányi. Mace-off23: Transferable machine learning force fields for organic molecules. *arXiv preprint arXiv:2312.15211*, 2023.
- [38] Georg Kresse and Jürgen Furthmüller. Efficient iterative schemes for ab initio total-energy calculations using a plane-wave basis set. *Physical review B*, 54(16):11169, 1996.
- [39] Georg Kresse and Jürgen Hafner. Ab initio molecular dynamics for liquid metals. *Physical review B*, 47(1):558, 1993.
- [40] Georg Kresse and Jürgen Hafner. Norm-conserving and ultrasoft pseudopotentials for first-row and transition elements. *Journal of Physics: Condensed Matter*, 6(40):8245, 1994.
- [41] Georg Kresse and Daniel Joubert. From ultrasoft pseudopotentials to the projector augmented-wave method. *Physical review b*, 59(3):1758, 1999.
- [42] Janice Lan, Aini Palizhati, Muhammed Shuaibi, Brandon M Wood, Brook Wander, Abhishek Das, Matt Uyttendaele, C Lawrence Zitnick, and Zachary W Ulissi. Adsorbml: a leap in efficiency for adsorption energy calculations using generalizable machine learning potentials. *npj Computational Materials*, 9(1):172, 2023.
- [43] Daniel S. Levine, Muhammed Shuaibi, Evan Walter Clark Spotte-Smith, Michael G. Taylor, Muhammad R. Hasyim, Kyle Michel, Ilyes Batatia, Gábor Csányi, Misko Dzamba, Peter Eastman, Nathan C. Frey, Xiang Fu, Vahe Gharakhanyan, Aditi S. Krishnapriyan, Joshua A. Rackers, Sanjeev Raja, Ammar Rizvi, Andrew S. Rosen, Zachary Ulissi, Santiago Vargas, C. Lawrence Zitnick, Samuel M. Blau, and Brandon M. Wood. The open molecules 2025 (omol25) dataset, evaluations, and models, 2025. URL <https://arxiv.org/abs/2505.08762>.
- [44] Yi-Lun Liao, Brandon Wood, Abhishek Das, and Tess Smidt. Equiformerv2: Improved equivariant transformer for scaling to higher-degree representations. *arXiv preprint arXiv:2306.12059*, 2023.
- [45] Antoine Loew, Dwen Sun, Hai-Chen Wang, Silvana Botti, and Miguel A. L. Marques. Universal Machine Learning Interatomic Potentials are Ready for Phonons, December 2024.
- [46] Andrea Madotto, Zhaojiang Lin, Chien-Sheng Wu, Jamin Shin, and Pascale Fung. Attention over parameters for dialogue systems. *NeurIPS Conversational AI Workshops*, 2020.
- [47] Saeed Masoudnia and Reza Ebrahimpour. Mixture of experts: a literature survey. *Artificial Intelligence Review*, 42:275–293, 2014.
- [48] Arslan Mazitov, Filippo Bigi, Matthias Kellner, Paolo Pegolo, Davide Tisi, Guillaume Fraux, Sergey Pozdnyakov, Philip Loche, and Michele Ceriotti. Pet-mad, a lightweight universal interatomic potential for advanced materials modeling, 2025. URL <https://arxiv.org/abs/2503.14118>.
- [49] Łukasz Mentel. mendelev - A Python package with properties of chemical elements, ions, isotopes and methods to manipulate and visualize periodic table., March 2021. URL <https://github.com/lmentel/mendelev>.
- [50] Frank Neese, Frank Wennmohs, Ute Becker, and Christoph Riplinger. The orca quantum chemistry program package. *The Journal of chemical physics*, 152(22), 2020.

- [51] Mark Neumann, James Gin, Benjamin Rhodes, Steven Bennett, Zhiyi Li, Hitarth Choubisa, Arthur Hussey, and Jonathan Godwin. Orb: A fast, scalable neural network potential. *arXiv preprint arXiv:2410.22570*, 2024.
- [52] Shyue Ping Ong, William Davidson Richards, Anubhav Jain, Geoffroy Hautier, Michael Kocher, Shreyas Cholia, Dan Gunter, Vincent L Chevrier, Kristin A Persson, and Gerbrand Ceder. Python materials genomics (pymatgen): A robust, open-source python library for materials analysis. *Computational Materials Science*, 68:314–319, 2013.
- [53] Yutack Park, Jaesun Kim, Seungwoo Hwang, and Seungwu Han. Scalable parallel algorithm for graph neural network interatomic potentials in molecular dynamics simulations. *J. Chem. Theory Comput.*, 20(11):4857–4868, 2024. doi: 10.1021/acs.jctc.4c00190.
- [54] Saro Passaro and C. Lawrence Zitnick. Reducing SO(3) convolutions to SO(2) for efficient equivariant GNNs. In *Proceedings of the 40th International Conference on Machine Learning*, volume 202. PMLR, 2023.
- [55] John P Perdew, Kieron Burke, and Matthias Ernzerhof. Generalized gradient approximation made simple. *Physical review letters*, 77(18):3865, 1996.
- [56] Balázs Póta, Paramvir Ahlawat, Gábor Csányi, and Michele Simoncelli. Thermal Conductivity Predictions with Foundation Atomistic Models, September 2024.
- [57] Raghunathan Ramakrishnan, Pavlo O Dral, Matthias Rupp, and O Anatole Von Lilienfeld. Quantum chemistry structures and properties of 134 kilo-molecules. *Scientific data*, 1(1):1–7, 2014.
- [58] Benjamin Rhodes, Sander Vandenhaute, Vaidotas Šimkus, James Gin, Jonathan Godwin, Tim Duignan, and Mark Neumann. Orb-v3: atomistic simulation at scale. *arXiv preprint arXiv:2504.06231*, 2025.
- [59] Janosh Riebesell, Rhys EA Goodall, Philipp Benner, Yuan Chiang, Bowen Deng, Alpha A Lee, Anubhav Jain, and Kristin A Persson. Matbench discovery—a framework to evaluate machine learning crystal stability predictions. *arXiv preprint arXiv:2308.14920*, 2023.
- [60] Carlos Riquelme, Joan Puigcerver, Basil Mustafa, Maxim Neumann, Rodolphe Jenatton, André Susano Pinto, Daniel Keysers, and Neil Houlsby. Scaling vision with sparse mixture of experts. *Advances in Neural Information Processing Systems*, 34:8583–8595, 2021.
- [61] Jonathan Schmidt, Tiago FT Cerqueira, Aldo H Romero, Antoine Loew, Fabian Jäger, Hai-Chen Wang, Silvana Botti, and Miguel AL Marques. Improving machine-learning models in materials science through large datasets. *Materials Today Physics*, 48:101560, 2024.
- [62] MD Segall, Philip JD Lindan, MJ al Probert, Christopher James Pickard, Philip James Hasnip, SJ Clark, and MC Payne. First-principles simulation: ideas, illustrations and the castepcode. *Journal of physics: condensed matter*, 14(11):2717, 2002.
- [63] Noam Shazeer, Azalia Mirhoseini, Krzysztof Maziarz, Andy Davis, Quoc Le, Geoffrey Hinton, and Jeff Dean. Outrageously large neural networks: The sparsely-gated mixture-of-experts layer. *arXiv preprint arXiv:1701.06538*, 2017.
- [64] Tomoya Shiota, Kenji Ishihara, Tuan Minh Do, Toshio Mori, and Wataru Mizukami. Taming multi-domain, -fidelity data: Towards foundation models for atomistic scale simulations, 2024. URL <https://arxiv.org/abs/2412.13088>.
- [65] Nima Shoghi, Adeesh Kolluru, John R Kitchin, Zachary W Ulissi, C Lawrence Zitnick, and Brandon M Wood. From molecules to materials: Pre-training large generalizable models for atomic property prediction. *arXiv preprint arXiv:2310.16802*, 2023.
- [66] Anuroop Sriram, Abhishek Das, Brandon M Wood, and C. Lawrence Zitnick. Towards training billion parameter graph neural networks for atomic simulations. In *International Conference on Learning Representations*, 2022. URL <https://openreview.net/forum?id=0jP2n0YFmKG>.

- [67] Anuroop Sriram, Sihoon Choi, Xiaohan Yu, Logan M Brabson, Abhishek Das, Zachary Ulissi, Matt Uyttendaele, Andrew J Medford, and David S Sholl. The open dac 2023 dataset and challenges for sorbent discovery in direct air capture, 2024.
- [68] Anuroop Sriram, Logan M. Brabson, Xiaohan Yu, Sihoon Choi, Kareem Abdelmaqsood, Elias Moubarak, Pim de Haan, Sindy Löwe, Johann Brehmer, John R. Kitchin, Max Welling, C. Lawrence Zitnick, Zachary Ulissi, Andrew J. Medford, and David S. Sholl. The open dac 2025 dataset for sorbent discovery in direct air capture, 2025. URL <https://arxiv.org/abs/2508.03162>.
- [69] Annika Stuke, Christian Kunkel, Dorothea Golze, Milica Todorović, Johannes T. Margraf, Karsten Reuter, Patrick Rinke, and Harald Oberhofer. Atomic structures and orbital energies of 61,489 crystal-forming organic molecules. *Scientific Data*, 7(1):58, February 2020. ISSN 2052-4463. doi: 10.1038/s41597-020-0385-y.
- [70] Hiteshi Tandon, Tanmoy Chakraborty, and Vandana Suhag. A brief review on importance of dft in drug design. *Res. Med. Eng. Sci*, 7(4):791–795, 2019.
- [71] Rithwik Tom, Timothy Rose, Imanuel Bier, Harriet O’Brien, Álvaro Vázquez-Mayagoitia, and Noa Marom. Genarris 2.0: A random structure generator for molecular crystals. *Computer Physics Communications*, 250:107170, 2020.
- [72] Richard Tran, Janice Lan, Muhammed Shuaibi, Brandon M Wood, Siddharth Goyal, Abhishek Das, Javier Heras-Domingo, Adeesh Kolluru, Ammar Rizvi, Nima Shoghi, et al. The open catalyst 2022 (oc22) dataset and challenges for oxide electrocatalysts. *ACS Catalysis*, 13(5): 3066–3084, 2023.
- [73] Alexander Urban, Dong-Hwa Seo, and Gerbrand Ceder. Computational understanding of li-ion batteries. *npj Computational Materials*, 2(1):1–13, 2016.
- [74] Hai-Chen Wang, Silvana Botti, and Miguel A. L. Marques. Predicting stable crystalline compounds using chemical similarity. *npj Computational Materials*, 7(1):1–9, January 2021. ISSN 2057-3960. doi: 10.1038/s41524-020-00481-6.
- [75] Mitchell Wortsman, Gabriel Ilharco, Samir Ya Gadre, Rebecca Roelofs, Raphael Gontijo-Lopes, Ari S Morcos, Hongseok Namkoong, Ali Farhadi, Yair Carmon, Simon Kornblith, et al. Model soups: averaging weights of multiple fine-tuned models improves accuracy without increasing inference time. In *International conference on machine learning*, pages 23965–23998. PMLR, 2022.
- [76] Hai Xiao, Jamil Tahir-Kheli, and William A Goddard III. Accurate band gaps for semiconductors from density functional theory. *The Journal of Physical Chemistry Letters*, 2(3):212–217, 2011.
- [77] Han Yang, Chenxi Hu, Yichi Zhou, Xixian Liu, Yu Shi, Jielan Li, Guanzhi Li, Zekun Chen, Shuizhou Chen, Claudio Zeni, Matthew Horton, Robert Pinsler, Andrew Fowler, Daniel Zügner, Tian Xie, Jake Smith, Lixin Sun, Qian Wang, Lingyu Kong, Chang Liu, Hongxia Hao, and Ziheng Lu. Mattersim: A deep learning atomistic model across elements, temperatures and pressures, 2024. URL <https://arxiv.org/abs/2405.04967>.
- [78] Naike Ye, Zekai Yang, and Yuchen Liu. Applications of density functional theory in covid-19 drug modeling. *Drug Discovery Today*, 27(5):1411–1419, 2022.
- [79] Duo Zhang, Xinzijian Liu, Xiangyu Zhang, Chengqian Zhang, Chun Cai, Hangrui Bi, Yiming Du, Xuejian Qin, Anyang Peng, Jiameng Huang, et al. Dpa-2: a large atomic model as a multi-task learner. *npj Computational Materials*, 10(1):293, 2024.
- [80] Alex Zunger, S.-H. Wei, L. G. Ferreira, and James E. Bernard. Special quasirandom structures. *Physical Review Letters*, 65(3):353–356, July 1990. doi: 10.1103/PhysRevLett.65.353.

Appendix Table of Contents

A Training Details and Hyperparameters	17
A.1 Two-stage training	17
A.2 Parallelisms	17
A.3 Model	17
A.4 MPtrj and sAlex Fine-tuning	18
A.5 Training Compute Resources	18
A.6 Referencing and Normalization	18
B Training Data	19
B.1 Materials	20
B.2 Molecules	20
B.3 Catalysis	20
B.4 Molecular Crystals	20
B.5 Metal-organic frameworks (MOFs)	20
C Scaling Laws Methods	21
C.1 FLOP counting	21
C.2 Compute optimal fits	21
C.3 Fitting loss vs. parameters	21
D Inference	22
E Evaluations	23
E.1 Additional UMA Results	24
E.2 Materials	24
E.3 Catalysis	25
E.4 Molecules	25
E.5 Molecular Crystals	27
E.6 Metal–Organic Frameworks	27
F Single-task vs Multi-task	28
G Additional MoLE Analysis	28
G.1 Expert Analysis	28
G.2 Generalization Across Architectures	28

A Training Details and Hyperparameters

A.1 Two-stage training

While conservative models have been found to provide reliable performance in diverse physical property prediction tasks [21], the backward pass required for force/stress prediction significantly increases inference costs. Models with direct force prediction are much more efficient, and have been found to be effective as a pre-training strategy to save compute when subsequently fine-tuned as a conservative model [21, 7]. The UMA-S and UMA-M both follow this procedure. In addition, we introduce low-precision training, max-atom batching, and max neighbor switching to further enhance the scalability and efficiency of our training process. These novel strategies are discussed in turn below. Detailed hyper-parameters are summarized in Table 4.

Precision. For pretraining, we used BF16 numerical format, commonly used in training LLMs but uncommon in MLIP models due to high numerical precision requirements. In our experiments, we found that BF16 is significantly more stable than AMP-FP16 (automatic mixed precision) especially in our multi-modal setting where data distributions can vary dramatically, frequently causing gradient and loss spikes that would destabilize AMP training. However, it suffers an accuracy drop compared to AMP-FP16 and FP32. We found the degradation can be nearly completely recovered after a very small number of finetuning steps in FP32 (<1% of data).

Max-atom Batching. Due to the large differences in system topology and number of atoms/edges per system, using a fixed number of systems as batch size is infeasible. Instead we chose to use a max-atom batching scheme where we randomly pack batches that contain as close to an upper bound (max atoms) as possible without going over to guarantee an upper bound on memory usage.

Max Neighbors. For training efficiency purposes, we use a significantly smaller number of neighbors per atom during pretraining and found that it has no effect on the final performance, energy conservation, and smoothness properties of the model after finetuning with effectively “infinite” max neighbors.

A.2 Parallelisms

Although our models are designed with inference efficiency in mind, training models with a large number of MoLE experts is memory intensive. In particular, for the finetuning stages, a combination of infinite neighbors, FP32 precision, and autograd forces puts significant constraints on memory and training speed. We used a combination three parallelism training techniques summarized as follows:

- Graph parallelism (GP) [66]: Partitioning graphs across GPUs during message passing layers is used when scaling up to a large number of atoms at large model sizes. Graph partitioning is only used within a node with a fixed graph parallel rank size (2 or 4) during conservative fine-tuning stages.
- Fully-sharded data parallel (FSDP): We use the Pytorch FSDPv1 implementation on MoLE expert layers only for models with a total parameter count exceeding 1B during conservative fine-tuning when memory is scarce. Parameters are sharded within a node and replicated across nodes.
- Distributed Data Parallel (DDP): We use the standard PyTorch DDP implementation, with modifications for per-atom loss averaging and compatibility with graph parallelism.

Furthermore, we leveraged Pytorch’s Distributed Checkpointing framework to ensure saving and loading extremely large checkpoints is efficient and stable across different node configurations. Exponential moving average (EMA) is used for stable validation performance.

A.3 Model

One model for all tasks. UMA is designed for multi-task learning under diverse DFT settings. For two inputs with exactly the same atomic numbers and positions, the DFT labels will be different when different DFT settings are used. Such DFT settings include the level of theory and system total charge/spin. These task specifications are global information of the atomic system, and we process them through initial embedding layers. In this paper, five levels of theories are involved –

Table 4: Summary of main training-related hyper-parameters for the pre-training and fine-tuning stages. These hyper-parameters are shared among model sizes.

Hyper-parameter	Pre-training	Finetuning
Precision	BF16	FP32
Radius cutoff Å	6	6
Max neighbors	30	300
Force prediction	Direct	Autograd
Stress prediction	None	Autograd
Optimizer	AdamW	AdamW
Learning rate scheduling	Cosine	Cosine
Maximum learning rate	8×10^{-4}	4×10^{-4}
Warmup epochs	0.01	0.01
Warmup factor	0.2	0.2
Gradient clipping norm threshold	100	100
Model EMA decay	0.999	0.999
Weight decay	1×10^{-3}	1×10^{-3}
Energy loss coefficient	10	20
OMol energy loss coefficient	30	-
Force loss coefficient	30	2
Stress loss coefficient	-	1

Table 5: Hyper-parameters for UMA models of different sizes.

Hyper-parameters	UMA-S	UMA-M	UMA-L
Number of MoLE experts	32	32	Dense
Number of layer blocks	4	10	16
Maximum degree L_{\max}	2	4	6
Maximum order M_{\max}	2	2	2
Number of channels N_{channel}	128	128	256
Number of radial basis functions	64	128	256
Global batch size (atoms)	88k	44k	44k
Number of pre-training steps	1.68M	2.08M	2.58M
Number of fine-tuning steps	1M	545k	350k

OMat24, OC20, OMol25, OMC25, and ODAC25 all use different DFT levels of theory. OMol25 further contains systems with non-neutral charge/spin.

For this iteration of the UMA models, these global information are embedded as follows:

Furthermore, to use a single model for all tasks, it is crucial to normalize the labels such that targets from different datasets fall into similar numerical ranges. We specifically design a referencing scheme that brings the diverse datasets to a similar level, detailed in Appendix B. The model hyperparameters are shown in Table 6.

A.4 MPtrj and sAlex Fine-tuning

For materials evaluations, UMA models were fine-tuned on the MPTrj [17] and sAlex [61, 5] datasets to ensure consistent DFT settings. The fine-tuning procedure is the same as eSEN-30M-OAM as documented in [21].

A.5 Training Compute Resources

The resources used to train UMA models are described in Table 7.

A.6 Referencing and Normalization

While each dataset used in this work comes with its own specific set of DFT settings, we wanted a referencing scheme that provides a way to make energy magnitudes comparable across datasets. We

Table 6: Hyper-parameters for UMA models of different sizes.

Hyper-parameters	UMA-S	UMA-M	UMA-L
Number of MoLE experts	32	32	Dense
Number of layer blocks	4	10	16
Maximum degree L_{\max}	2	4	6
Maximum order M_{\max}	2	2	2
Number of channels N_{channel}	128	128	256
Number of radial basis functions	64	128	256
Global batch size (atoms)	88k	44k	44k
Number of pre-training steps	1.68M	2.08M	2.58M
Number of fine-tuning steps	1M	545k	350k

Table 7: Training Times for UMA models.

Model	Stage	GPUs in Parallel	Training Days	GPU-Type
UMA-S	Direct Pre-train	128	5	H200 140GB
UMA-S	Conserve Fine-tune	256	5	H200 140GB
UMA-M	Direct Pre-train	128	14	H200 140GB
UMA-M	Conserve Fine-tune	256	14	H200 140GB
UMA-L	Direct Pre-train	128	25	H100 80GB
UMA-L	Stress Fine-tune	128	4	H100 80GB
UMA-L	FP32 Fine-tune	128	2	H100 80GB

do this through a "heat of formation" (HOF) reference that is applied to the energies:

$$E_{ref} = E_{DFT} - \sum_i^N [E_{i,DFT} - \Delta H_{f,i}]$$

Where E_{DFT} corresponds to the total DFT energy of the system, i is the atom number, N is the total number of atoms in the system, $E_{i,DFT}$ is the DFT energy of an isolated atom i in a box, and $\Delta H_{f,i}$ is the heat of formation of atomic number i as taken directly from Mendeleev [49]. $E_{i,DFT}$ was calculated using the DFT settings for each of the unique datasets in this work. Additionally, we apply a linear reference to the above energies to help with the convergence and training stability of our models. We follow the same protocol as described in the OC22 Appendix [72].

We use a custom normalization $x' = \frac{x-\mu}{\sigma}$ for all targets (energy, forces, stress), where the shift term $\mu = 0$ and the scale term $\sigma = \text{Force root mean square (RMS)}$. For the combined dataset the Force RMS is computed as the weighted average (based on the number of systems) of all individual dataset Force RMS values.

B Training Data

A summary of the five datasets used to train UMA is shown in Table 8. In total, the dataset has 459 million training examples, containing up to 350 atoms. The average number of atoms varies based on the dataset, from 19 for OMat24 to 178 for ODAC25.

Table 8: Overview of the five datasets used to train UMA. For each dataset various statistics are provided alongside the sampling ratio used for training.

Dataset	Domain	Training Size	Labels	# Elements	Avg Size	Force RMS	Sampling ratio
OMat24	Materials	100,824,585	E,F,S	89	19	2.83	4
OMol25	Molecules	75,889,983	E,F	83	52	0.985	4
OC20++	Catalysis	229,054,043	E,F	56	77	0.624	1
OMC25	Molecular Crystals	24,870,226	E,F,S	12	130	0.103	2
ODAC25	MOFs	28,517,826	E,F	70	178	0.046	1
Total		459,156,663					

B.1 Materials

The field of inorganic bulk materials is moving at an incredibly fast pace. Here we train on the Open Materials (OMat24) dataset (100M) [5], one of the largest and most diverse datasets in the community. All DFT calculations from this domain were run with VASP [39, 38, 40, 41] and used the PBE [55] functional. Due to the differences in pseudopotential version and different pseudopotentials for certain elements in OMat24 and Materials Project [5] calculation settings used for the data in most third party benchmarks, finetuning was also performed on MPtrj [17] and subsampled Alexandria (sAlex) [61] to ensure consistent evaluation on the materials benchmarks.

B.2 Molecules

The community has seen dozens of molecular datasets spanning different scales for a variety of applications []. However, the varying levels of DFT theory and quality makes it challenging to unify under a single model. The release of the Open Molecules 2025 (OMol25) dataset [43] helps address this by providing the largest single dataset (100M+) spanning 80+ elements covering metal-complexes, biomolecules, electrolytes, and several existing datasets under a single, high-quality level of theory. All DFT calculations were performed using Orca [50] (ω B97M-V/def2-TZVPD). At the time of training, only 75M samples from OMol25 were available for use, and we refer to this as OMol-preview. Splits were constructed to ensure that this snapshot of the dataset is consistent with the full dataset release. All ablations and results were trained with this OMol-preview, unless stated otherwise. Released models, however, will be retrained with the full OMol25 dataset to ensure the best models are accessible by the community.

B.3 Catalysis

The Open Catalyst (OC20) dataset [11] provides the largest adsorbate+surface dataset in the community. OC20 enumerates 1M+ unique surface + adsorbate combinations, spanning 55 elements, and runs local geometry optimizations. Here, we train on the OC20 All (133M), MD (38M), and Rattled (17M) datasets. Unlike prior work, we also leverage OC20’s clean surface data (14M) since models here are trained on total energies. One limitation of OC20 is that it only contains single adsorbates that interact with a surface. To address this, we introduce the OC20-Multi-Adsorbate (mAds) dataset (22M) to better capture coverage effects and adsorbate-adsorbate interactions. All DFT calculations were performed using VASP [39, 38, 40, 41] with the RPBE exchange-correlation functional [26].

B.4 Molecular Crystals

The most recent 7th Crystal Structure Prediction (CSP) Blind Test organized by Cambridge Crystallographic Data Center (CCDC) demonstrated the effectiveness of tailored machine learning interatomic potentials (MLIPs) in predicting, filtering, and ranking molecular crystal structures [30, 29]. However, despite the widespread applications of molecular crystals, there has been limited focus on developing universal MLIPs for molecular crystals, mostly because of the scarcity of publicly available datasets. Currently, publicly available datasets of molecular crystals are scarce, with at most 60,000 materials represented [3, 9]. To address this data gap, we use the Open Molecular Crystals (OMC25) dataset, which comprises 25 million molecular crystal structures. The dataset includes multiple relaxation trajectories of various molecular crystal packings generated with Genarris [71] starting from organic molecules from the OE62 dataset [69]. The dataset includes 12 elements (all elements from OE62, excluding Li, As, Se, and Te) and the maximum number of atoms is capped at 300. The dataset is computed using VASP [39, 38, 40, 41] with the PBE exchange-correlation functional [55] and D3 dispersion correction [25]. The OMC25 dataset, along with in-depth details on data and polymorph structure generation, will be released in an upcoming publication [23].

B.5 Metal-organic frameworks (MOFs)

The Open Direct Air Capture 2025 (ODAC25) dataset represents the largest MOF dataset (78M) for DAC applications [68]. ODAC25 extends the earlier ODAC23 [67] dataset, and is derived from the CoREMOF [13, 14] dataset. ODAC25 focuses on the adsorption and co-adsorption of CO₂ and H₂O in MOFs among other adsorbates, which is critical for DAC performance evaluation. This work uses

the subset of ODAC25 that overlaps with ODAC23, where all DFT-computed adsorption energies have been upgraded to a higher k-points sampling grid density, providing improved accuracy over ODAC23 (29M calculations). All DFT calculations were performed using VASP [39, 38, 40, 41] with the PBE exchange-correlation functional [55] and D3 dispersion correction [25].

C Scaling Laws Methods

The scaling law experiments were only performed on pretraining; due to compute constraints, we did not study the effect on finetuning with energy conservation. We used an 8-expert MoLE version of the model with the UMA-M settings ($l_{max} = 4$, $m_{max} = 2$, and $n_{neighbors} = 30$) for consistency.

C.1 FLOP counting

We approximate our training FLOPs by

$$C(N, D) \approx \kappa ND, \tag{3}$$

where N is the total number of parameters in the network, and D is the number of inputs (tokens for LLMs and atoms or edges for MLIPs) computed on. This relationship holds for any network that is dominated by linear layers where κ indicates how many times a parameter is re-used on an input. For a single forward pass of a linear network, $\kappa = 2$. A full training cycle for such a network with a single backward pass brings $\kappa = 6$ as we need to compute the gradient with respect to both the parameters and inputs. Thus, for most LLMs $\kappa = 6$ FLOPs/parameter/token [35] for a single forward and backwards pass where D is in units of tokens.

For our edge-based SO2 equivariant networks [54], κ is a function of l_{max} and m_{max} spherical harmonic orders and the number of edges per atom $n_{neighbors}$. For the scaling law experiments, we used $l_{max} = 4$, $m_{max} = 2$, and $n_{neighbors} = 30$ which corresponds to the settings of UMA-M model, resulting in $\kappa \approx 270$ FLOPs/parameter/atom (or 9 FLOPs/parameter/edge) per training step, which can be computed or experimentally determined. As long as the number of input edges and parameters are sufficiently large (which holds for UMA models), this flop approximation holds as contributions from all other operators are marginal. We also verified this assumption with direct FLOP counting in our model code.

Overall, parameter reuse is significantly higher in Equivariant-GNNs compared to LLMs, and hence the flop count is 2-3 orders of magnitude higher for a similar parameter-sized LLM network.

C.2 Compute optimal fits

The compute optimal model and dataset sizes can then be fitted to power laws [35, 28]:

$$\begin{aligned} \log(N^*(C)) &= \alpha \log(C) + A \\ \log(D^*(C)) &= \beta \log(C) + B \end{aligned} \tag{4}$$

Where C is the compute in FLOPs described in Appendix C.1. $N^*(C)$ represents the optimal model size (in parameters) as a function of compute, and $D^*(C)$ represents the optimal dataset size (in units of atoms). $N^*(C)$ is determined by finding the minima of fitted parabolas for each Isoflop curve. The 10% and 90% percentile bootstrap errors are shown in Figure 3(e). α and β are the scaling coefficients w.r.t. model size and dataset size respectively. A and B are offset constants of the fit. Fit coefficients and bootstrap errors are shown in Table 9.

C.3 Fitting loss vs. parameters

To understand the minimum achievable loss for dense vs MoLE models we can fit the more general parameterized ansatz of $L(N, D)$ proposed by [35].

$$\tilde{L}(N, D) = \hat{E} + \frac{\hat{A}}{N^{\hat{\alpha}}} + \frac{\hat{B}}{D^{\hat{\beta}}} \tag{5}$$

This maps the power law coefficients from Equation 5 to those in Equation 4 by using $\alpha = \frac{\hat{\beta}}{\hat{\alpha} + \hat{\beta}}$ and $\beta = \frac{\hat{\alpha}}{\hat{\alpha} + \hat{\beta}}$. Here we can either minimize the $\tilde{L}(N, D)$ directly by fitting the 5 parameters $\hat{E}, \hat{A}, \hat{B}, \hat{\alpha}, \hat{\beta}$ with a iterative minimization procedure such as LBFGS [28, 10] or by examining the loss as a power relationship of N^* using

$$\log \tilde{L}(N^*) = \hat{\alpha} \log(N^*) + \gamma \quad (6)$$

where $\gamma = \log([1 + \frac{\hat{\alpha}}{\hat{\beta}}]\hat{A})$ with $\hat{E} \approx 0$. We found both methods yielded similar results but the minimization of \tilde{L} was more sensitive to the choice of hyperparameters.

Table 9: Power Law Coefficients determined from fitting Equations 4 and 6. Error bounds are determined by bootstrap sampling 1000 times and taking the 10th and 90th percentile values, quoted in brackets.

Parameter	Dense	MoLE
α	0.61 (0.57,0.65)	0.56 (0.49,0.59)
β	0.39 (0.35, 0.43)	0.44 (0.39, 0.43)
A	-4.5 (-3.8, -5.3)	-3.8 (-2.56, -4.65)
B	3.6 (2.9, 4.4)	2.9 (1.6, 3.7)
$\hat{\alpha}$	-0.29 (-0.27, -0.31)	-0.25 (-0.2, -0.3)
γ	2.16 (2.02, 2.34)	1.82 (1.61, 2.12)

D Inference

For inference benchmarking we use a periodic fcc carbon system with lattice constant $a = 3.8\text{\AA}$. This results in a fixed density of approximately 50 edges per atom within 6\AA . For UMA models, we use a combination of torch.compile, cuda graphs and pre-merged MoLE experts for inference speed. For large number of atoms (> 1000), we use edge-based activation checkpointing to trade off memory for some speed, allowing us to fit 100k+ atoms for the UMA-S into memory. We checked all our optimizations chosen does not degrade simulation accuracy, equivariance or energy conservation properties. While our benchmarks do not include graph generation, our internal CUDA based graph generation algorithm is very fast and decreases throughput by no more than 10% even for the largest systems tested. In the case of non-MoLE merging, we found the inference speed was comparable but the parameters require more GPU memory to store.

Table 10: Single-GPU simulation speeds for energy-conservative models in *steps per second*: comparing conservative UMA models to the top two models (eSEN and OrbV3) on the Matbench Discovery leaderboard [59] and the MACE materials and molecules models. Benchmarks are run, excluding graph generation, on a single Nvidia H100 80GB GPU using FP32 (TF32-high precision) and torch compile when possible. Test systems are a standard periodic atomic system that have ≈ 50 neighbors per atom with a 6\AA cutoff. OOM indicates the model ran out of memory. Refer to Sec.D for more details.

Atoms	UMA-S (6.6M)	UMA-M (50M)	eSEN-30M- OAM (30M)	Orb-v3 conservative- inf-omat (25M)	MACE- MPA-0 (9M)	MACE- OFF23-L (4.7M)
100	44	21	8	77	38	89
1,000	16	3	1.7	30	24	20
10,000	1.6	0.2	OOM	3.7	2.9	OOM
50,000	0.2	OOM	OOM	OOM	OOM	OOM
100,000	0.1	OOM	OOM	OOM	OOM	OOM

For fair comparisons against other models, we used pytorch2.6.0, cuda12.4, python3.12 and TF-32 precision universally on a H100 80GB GPU. We use standard torch.compile settings whenever possible (only MACE-MPA-0 failed to compile). Different models have different radius cutoffs and

max neighbors settings. We made sure that all models was receiving roughly 50 neighbors per atom for the same number of atoms.

E Evaluations

Section E.1 provides results for all versions of UMA.

Sections E.2-E.6 provides additional results for the original version of UMA, which was trained on a preview subset of the OMol25 dataset.

Table 11: Test MAE results on held out test splits for materials [59], catalysis [11], molecules [43], molecular crystals [23] and MOFs [67]. All energies are in meV, forces are in meV/Å and stresses are in meV/Å³. Results for UMA are compared against the SOTA literature results. Target accuracies for practical utility are provided as an approximate guide for reference.

Model	Materials						Catalysis				Molecules				Molecular crystals			MOFs	
	WBM Energy/Atom	Forces	Stress	HEA Energy/Atom	Forces	Stress	ID Ads. Energy	Forces	OOD-Both Ads. Energy	Forces	OOD-Comp Energy/Atom	Forces	PDB-TM Energy/Atom	Forces	OMC-Test Energy/Atom	Forces	Stress	OOD-LT Ads. Energy	Forces
UMA																			
UMA-S	20.0	60.8	4.4	22.0	72.8	3.1	52.1	24.3	70.2	30.9	3.64	10.80	0.88	16.12	0.91	4.77	0.97	292.4	16.0
UMA-M	18.1	51.4	4.3	19.0	62.2	3.2	33.4	16.0	46.5	21.0	3.26	9.09	0.69	10.37	0.82	3.00	0.98	290.2	10.7
UMA-L	17.6	45.5	3.8	24.8	48.3	2.8	32.4	12.2	43.5	15.9	2.33	5.19	0.81	8.76	0.59	2.28	0.10	291.1	6.5
UMA-S-1	19.4	62.2	4.5	21.9	73.5	3.1	53.1	24.5	70.4	31.2	0.96	8.25	0.93	15.56	0.93	5.15	1.01	287.1	13.6
UMA-S-1.1	20.2	62.8	4.4	24.9	83.7	3.5	51.5	24.1	68.8	30.7	0.95	8.64	0.84	15.47	1.03	5.04	0.93	289.9	13.3
UMA-M-1.1	18.2	50.7	4.2	21.9	69.0	3.5	31.8	15.5	45.5	20.2	0.74	5.44	0.50	10.14	0.84	2.83	0.90	294.1	10.3
Literature																			
eSEN-OMat [21]	16.2	49.6	4.1	20.0	59.5	3.2	-	-	-	-	-	-	-	-	-	-	-	-	-
eqV2-OMat [5]	14.9	46.3	3.6	20.3	47.0	2.7	-	-	-	-	-	-	-	-	-	-	-	-	-
eqV2-OC20 [44]	-	-	-	-	-	-	149.1	11.6	306.5	15.7	-	-	-	-	-	-	-	-	-
GemNet-OC20 [22]	-	-	-	-	-	-	163.5	16.3	343.3	23.1	-	-	-	-	-	-	-	-	-
eSEN-sm-cons. [43]	-	-	-	-	-	-	-	-	-	-	1.35	7.39	0.83	12.72	-	-	-	-	-
eSEN-S-OMC [23]	-	-	-	-	-	-	-	-	-	-	-	-	-	-	1.05	5.39	0.94	-	-
eqv2-ODAC [67]	-	-	-	-	-	-	-	-	-	-	-	-	-	-	-	-	-	316.0	7.2
Target																			
Practical Utility	10-20	-	-	10-20	-	-	100	-	100	-	1-3	-	1-3	-	1-3	-	-	100	-

Table 12: Evaluation results on Matbench-Discovery [59], MDR phonon [45], elastic tensor [16, 34], and AdsorbML benchmarks [42]. Results are also provided for a diverse set of molecule [43] and molecular crystal [29, 23] benchmarks. NVE MD [21] tests whether energy conservation is observed when running the model for molecular dynamics. SOTA results from literature are reported where available. For the materials evaluations, UMA models were fine-tuned on MPtrj [17] and sAlex [61, 5] to be consistent with the benchmark’s DFT settings.

Model	Materials								Catalysis	Molecules				Molecular Crystals				
	Matbench [59] F1	RMSD	MAE [eV/atom]	κ_{syme} [56]	Phonons [45] ω_{max} [K]	Free Energy [kJ/mol]	Elasticity [16, 34] G_{vrb} [GPa]	K_{vrb} [GPa]		NVE MD [21] Conserve	AdsorbML [42] Success Rate	OMol25 [43] Ligand-strain [meV]	PDB-pocket [meV]	Dist-SR [meV]	Dist-LR [meV]	NVE MD [21] Conserve	CSP Targets [29] Lattice Energy [kJ/mol]	Kendall Rank
UMA																		
UMA-S	0.916	0.064	0.020	0.203	17.59	5.00	8.54	4.96	✓	68.35%	4.39	150.3	67.6	432.1	✓	2.695	0.82	0.12
UMA-M	0.930	0.061	0.018	0.195	13.91	3.39	8.40	4.76	✓	71.12%	2.45	89.7	41.6	588.7	✓	2.664	0.81	0.13
UMA-L	0.928	0.065	0.018	0.671	78.50	18.20	20.56	14.48	✗	74.41%	3.37	71.7	16.6	246.1	✗	2.488	0.84	0.12
UMA-S	0.916	0.064	0.020	0.203	17.59	5.0	8.54	4.96	✓	68.35%	4.39	150.3	67.6	432.1	✓	2.70	0.82	0.12
UMA-S-1	0.914	0.064	0.020	0.231	18.65	5.51	13.72	5.19	✓	64.85%	5.19	138.3	23.8	-	✓	2.57	0.81	0.13
UMA-S-1.1	0.913	0.064	0.020	0.204	18.82	5.48	9.47	5.16	✓	66.80%	5.2	127.7	26.7	256.7	✓	2.13	0.86	0.13
UMA-M-1.1	0.929	0.061	0.018	0.176	14.81	3.87	8.57	4.78	✓	72.25%	2.3	76.8	21.5	214.8	✓	3.24	0.82	0.14
Literature																		
eSEN-30M-OAM [21]	0.925	0.061	0.018	0.170	15.00	4.00	9.13	5.73	✓	-	-	-	-	-	-	-	-	-
ORB v3 [58]	0.905	0.075	0.024	0.210	-	-	-	-	-	-	-	-	-	-	-	-	-	-
SevenNet-MF-ompa [36]	0.901	0.064	0.021	0.317	-	-	-	-	-	-	-	-	-	-	-	-	-	-
GRACE-2L-OAM [8]	0.880	0.067	0.023	0.294	-	-	-	-	-	-	-	-	-	-	-	-	-	-
MACE-MPA-0 [6]	0.852	0.073	0.028	0.412	-	-	-	-	-	-	-	-	-	-	-	-	-	-
eqv2-OC20 [42]	-	-	-	-	-	-	-	-	-	60.80%	-	-	-	-	-	-	-	-
GemNet-OC20 [42]	-	-	-	-	-	-	-	-	-	54.88%	-	-	-	-	-	-	-	-
eSEN-sm-cons. [43]	-	-	-	-	-	-	-	-	-	-	4.52	147.3	28.6	268.6	✓	-	-	-
eSEN-S-OMC [23]	-	-	-	-	-	-	-	-	-	-	-	-	-	-	-	6.18	0.74	0.18

E.1 Additional UMA Results

In this section, we provide results for the UMA, UMA-1, and UMA-1.1 models. The original UMA models (S, M, L) were trained on a preview subset of the OMol25 dataset ($\approx 70\%$), since portions of the dataset were still being calculated when UMA model training began. Both UMA-1 and UMA-1.1 were trained on the full OMol25 as released 05/14/2025. The other datasets used for training were unchanged, with the exception of the sampling ratios (Table 8) where the OMat24 coefficient was changed from 4 to 2 for both UMA-1 and UMA-1.1. UMA-1.1 resolved a size extensive bug later discovered. These models were fine-tuned on our 1.0 models with the fix in place. Tables 11 and 12 correspond to Tables 2 and 3 in the main text. Additional UMA 1 series models will be included in the arXiv version of the paper.

E.2 Materials

Table 13: Materials validation and test evaluations from OMat24 [5] and HEA. All energies are in meV, forces are in meV/Å and stresses are in meV/Å³.

Model	Val [5]				WBM [5]			OOD Composition [5]			OOD Element [5]			HEA		
	Energy/Atom	Forces	Stress	Force Cosine	Energy/Atom	Forces	Stress	Energy/Atom	Forces	Stress	Energy/Atom	Forces	Stress	Energy/Atom	Forces	Stress
UMA																
UMA-S	11.3	57.1	2.9	0.98	20.0	60.8	4.4	11.5	57.0	3.0	9.9	56.9	2.6	22.0	72.8	3.1
UMA-M	10.0	47.3	2.7	0.99	18.1	51.4	4.3	10.2	47.6	2.9	8.5	47.1	2.4	19.0	62.2	3.2
UMA-L	9.7	43.5	2.5	0.99	17.6	45.5	3.8	9.8	43.6	2.6	8.1	43.6	2.3	24.8	48.3	2.8
Literature																
eSEN-30M-OMat [21]	10.7	47.3	2.6	0.99	16.2	49.6	4.1	10.7	47.3	2.8	9.0	47.2	2.3	20.0	59.5	3.2
eqV2-86M-OMat [44]	10.0	44.9	2.4	0.99	14.9	46.3	3.6	10.0	44.5	2.5	8.8	44.7	2.1	20.3	47.0	2.7

Table 14: **Materials evals results.** We note that UMA models are fine-tuned on the MPTrj [17] and sAlex [61, 5] datasets to be consistent with the DFT settings of the benchmarks.

Model	Matbench [59]				Kappa 103 [56]				MDR Phonons [45]				Elasticity [16, 34]		Binary Elasticity		NVE MD [21]		
	F1	DAF	Precision	Accuracy	MAE [eV/atom]	RMSE [eV/atom]	r ²	κ_{src}	κ_{srne}	ω_{max} , MAE [K]	ω_{sig} , MAE [K]	Entropy, MAE [kJ/K/mol]	C_v , MAE [kJ/K/mol]	Free Energy, MAE [kJ/mol]	G_{vib} , MAE [GPa]	K_{vib} , MAE [GPa]	G_{vib} , MAE [GPa]	K_{vib} , MAE [GPa]	Conservative
UMA																			
UMA-S	0.92	6.00	0.92	0.97	0.02	0.07	0.87	0.09	0.20	17.59	7.41	13.59	3.49	5.00	8.54	4.96	8.57	5.25	✓
UMA-M	0.93	6.08	0.93	0.98	0.02	0.07	0.87	0.09	0.20	13.91	5.11	9.63	2.66	3.39	8.40	4.76	7.07	4.75	✓
UMA-L	0.93	6.09	0.93	0.98	0.02	0.07	0.86	0.45	0.67	78.50	27.68	43.04	15.85	18.20	20.56	14.48	21.95	17.01	✗
Literature																			
eSEN-30M-OAM [21]	0.93	6.07	0.93	0.98	0.02	0.07	0.87	-	0.17	15.00	10.21	10.00	3.00	4.00	9.13	5.73	9.02	5.73	✓
eqV2-86M-OAM [5]	0.92	6.05	0.92	0.98	0.02	0.07	0.85	1.82	1.94	840.33	377.96	426.79	102.72	251.14	19.60	26.25	22.02	26.50	✗

Full results on materials’ benchmarks are in Tables 13 and 14. Table 13 shows both validation and test results following OMat24 [5] along with the new high entropy alloy HEA test introduced in this paper. The HEA dataset contains relaxation trajectories for over 5000 alloys with atomic configuration disorder. Input structures were generated by sampling metallic element combinations of up to 6 different unique elements and using the special quasirandom structure method [80, 4] to decorate face-centered cubic, body-centered cubic and hexagonal close packed structures. DFT relaxations were carried out following the settings used in the OMat24 dataset [5].

In Table 14 we show full results for Matbench discovery [59], MDR phonon, elastic tensors, high entropy alloy IS2RE and NVE MD conservation benchmarks. The Matbench-Discovery benchmark evaluates a model’s ability to predict ground-state thermodynamic stability by optimizing geometry and predicting energy. The thermal conductivity prediction task demands accurate modeling of harmonic and anharmonic phonons, which are crucial for precise predictions of thermal transport. The MDR Phonon benchmark assesses a model’s performance in predicting phonon and vibrational thermodynamic properties. The MP elastic constant benchmark tests a model’s accuracy in predicting

bulk and shear moduli, requiring precise calculations of stress tensors and their derivatives with respect to cell deformations.

E.3 Catalysis

For catalysis, we show full validation and test results for OC20 [11] in Table 15. The structures in the dataset contain molecules, called adsorbates, interacting with surfaces. The goal is to estimate the adsorption energy, which is the change in energy as the adsorbates come into contact with the surface, and the forces on the atoms. Force MAEs are comparable across UMA-M and UMA-L to other state-of-the-art models. Adsorption energies for UMA are calculated by subtracting two total energy calculations as described in the main text, which improves results over prior models.

In addition to energy and forces MAEs, we use AdsorbML to evaluate the performance on the practically relevant task of finding the global minima adsorption energy [42]. One limitation of the originally proposed AdsorbML pipeline is that it requires a DFT evaluation of the ML-identified global minima structure. To make this benchmark more accessible to those without access to DFT, we propose a slightly altered version of this benchmark that only requires ML. Here, we follow the same AdsorbML pipeline but allow the use of the ML-predicted global minima energy, but success is now only considered if the energy is within 0.1 eV of the DFT minima. Previously, success did not enforce a lower bound so long a DFT evaluation confirmed that energy prediction is realized. Without DFT, we also set a lower bound of 0.1 eV to provide some flexibility to finding a better global minima than DFT. We show that metrics are still highly correlated when you perform the original evaluation to the one proposed here.

Table 15: Catalysis validation and test results on OC20 [11] metrics. All energies are in meV and forces are in meV/Å.

Model	Val (Total Energy)						Test (Ads. Energy)			
	ID			OOD-Both			ID		OOD-Both	
	Energy	Forces	Force Cosine	Energy	Forces	Force Cosine	Energy	Force	Energy	Force
UMA										
UMA-S	63.6	24.1	0.63	107.0	29.2	0.65	52.1	24.3	70.2	30.9
UMA-M	43.1	15.8	0.73	70.0	19.2	0.75	33.4	16.0	46.5	21.0
UMA-L	32.6	12.0	0.77	49.8	14.5	0.79	32.4	12.2	43.5	15.9
Literature										
eqV2-OC20 [44]	-	-	-	-	-	-	149.1	11.63	306.5	15.74
GemNet-OC20 [22]	-	-	-	-	-	-	163.5	16.33	343.3	23.11

E.4 Molecules

Table 16: Open Molecule 2025 [43] validation evaluations across biomolecules, electrolytes, metal complexes, neutral organics and OOD-comp. All energies are in meV and forces are in meV/Å. All models are trained with preview OMol25.

Model	Biomolecules		Electrolytes		Metal Complexes		Neutral Organics		OOD-Comp	
	Energy/Atom	Force	Energy/Atom	Force	Energy/Atom	Force	Energy/Atom	Force	Energy/Atom	Force
	UMA									
UMA-S	0.53	5.69	2.69	11.65	4.63	37.85	1.00	13.15	3.62	12.02
UMA-M	0.44	3.95	2.28	10.21	3.60	28.81	0.68	7.00	3.21	9.90
UMA-L	0.33	2.90	1.13	4.52	3.35	24.85	0.65	5.02	2.39	5.83
Baseline										
eSEN-S-OMol	0.54	6.06	2.52	12.63	4.27	37.30	0.84	13.00	3.69	12.78

We report results on molecules following the Open Molecules 2025 [43]. These include energy and force estimates for validation and test splits, as well as, numerous other tasks. The validation and test results are shown in Tables 16 and 17, respectively. Note that the eSEN-S-OMol model is only trained on the preview OMol25 dataset, which is $\approx 70\%$ of the full OMol25 dataset for a fair

Table 17: Open Molecule 2025 [43] test evaluations across biomolecules, electrolytes, metal complexes, neutral organics and OOD-comp, metal ligand, PDB-TM, reactivity, COD and anions. All energies are in meV and forces are in meV/Å. All models are trained with preview OMol25.

Model	Biomolecules		Electrolytes		Metal Complexes		Neutral Organics		OOD-Comp		Metal Ligand		PDB-TM		Reactivity		COD		Anions	
	Energy/Atom	Force	Energy/Atom	Force	Energy/Atom	Force	Energy/Atom	Force	Energy/Atom	Force	Energy/Atom	Force	Energy/Atom	Force	Energy/Atom	Force	Energy/Atom	Force	Energy/Atom	Force
UMA																				
UMA-S	0.51	5.70	3.80	13.95	3.07	33.56	1.49	20.33	3.64	10.80	1.23	17.71	0.88	16.12	4.82	61.80	2.92	29.82	0.66	10.85
UMA-M	0.42	3.89	3.29	13.19	2.40	24.85	0.98	10.83	3.26	9.09	0.99	12.04	0.69	10.37	3.88	47.75	2.19	20.11	0.50	8.03
UMA-L	0.34	2.92	1.41	5.42	2.47	21.67	1.03	6.91	2.33	5.19	1.05	10.00	0.81	8.76	3.93	41.97	2.57	15.44	0.62	5.90
Baseline																				
eSEN-S-OMol	0.52	6.06	3.52	15.23	2.86	33.30	1.35	20.06	3.67	11.56	1.18	17.49	0.79	14.11	4.89	61.16	2.93	24.12	0.47	10.38

comparison with the UMA models that were trained on the same subset. In general, the UMA-S and eSEN-S-OMol models provide comparable results.

Table 18: Open Molecule 2025 [43] single point evaluations for protein-ligand, IE/EA, spin gap and distance scaling. All energies are in meV and forces are in meV/Å. All models are trained with preview OMol25.

Model	Protein-ligand		IE/EA			Spin gap			Distance scaling			
	Ex Energy MAE	Ex Forces MAE	Δ Energy MAE	Δ Forces MAE	Δ Forces cosine sin.	Δ Energy MAE	Δ Forces MAE	Δ Forces cosine sin.	Δ Energy (SR) MAE	Δ Forces (SR) MAE	Δ Energy (LR) MAE	Δ Forces (LR) MAE
UMA												
UMA-S	150.25	5.09	336.16	80.60	0.77	665.75	112.09	0.69	67.60	4.11	432.14	5.54
UMA-M	89.69	4.06	236.76	66.28	0.81	547.73	98.15	0.74	41.60	3.86	588.74	8.73
UMA-L	71.68	2.27	244.23	57.18	0.82	568.36	93.09	0.73	16.55	2.03	246.10	2.34
Baselines												
eSEN-S-OMol	154.48	5.59	310.19	77.48	0.77	634.02	110.28	0.70	73.02	4.16	608.91	7.69

Table 19: Open Molecule 2025 [43] optimization evaluations including ligand-strain, conformer prediction, and protonation states. Results are reported across a variety of energy and structure based metrics for each task. All energies are in meV. All models are trained with preview OMol25.

Model	Ligand strain			Conformers				Protonation			
	Strain energy MAE [meV]↓	RMSD min. [Å] ↓	RMSD ensemble [Å] ↓	RMSD boltz. [Å] ↓	Δ Energy MAE [meV] ↓	RMSD reopt. [Å] ↓	Δ Energy reopt. [meV] ↓	RMSD ensemble [Å] ↓	Δ Energy MAE [meV] ↓	RMSD reopt. [Å] ↓	Δ Energy reopt. [meV] ↓
UMA											
UMA-S	4.39	0.28	0.06	0.05	5.76	0.02	3.06	0.13	40.42	0.04	18.35
UMA-M	2.45	0.19	0.04	0.03	3.19	0.01	1.47	0.08	24.08	0.02	10.99
UMA-L	3.37	0.25	0.05	0.05	4.97	0.01	2.27	0.11	30.31	0.02	12.54
Baselines											
eSEN-S-OMol	5.15	0.31	0.06	0.05	5.25	0.03	3.24	0.13	32.82	0.04	18.65

OMol25 [43] provides numerous other tasks for evaluation. These include evaluations which only require the estimation of a single point DFT calculation and evaluations that require optimizations. The comparison for single point DFT calculations is shown in Table 18. Similar to the test results, the UMA-S and eSEN-S-OMol models perform similarly with the UMA-M and UMA-L performing significantly better. Table 19 shows the results for tasks that require optimizations, which require repeated calls to the model to update atoms positions until a local energy minima is found. The small models report similar performance, and the UMA-M demonstrates the highest accuracies. It is likely that UMA-M outperforms UMA-L due to UMA-M being energy conserving and better behaved during optimization tasks.

Table 20: Open Molecular Crystals 2025 [23] validation and test table. All energies are in meV, forces are in meV/Å and stresses are in meV/Å³.

Model	Val				Test			
	Energy/Atom	Forces	Stress	Force Cosine	Energy/Atom	Forces	Stress	Force Cosine
UMA								
UMA-S	0.9	4.9	1.0	0.92	0.9	4.8	1.0	0.93
UMA-M	0.8	3.1	1.0	0.95	0.8	3.0	1.0	0.95
UMA-L	0.6	2.3	0.1	0.96	0.6	2.3	0.1	0.96
Baselines								
eSEN-S-OMC	1.06	5.58	0.96	0.92	1.05	5.39	0.94	0.92

Table 21: Open Molecular Crystals 2025 [23] evaluation for polymorphs from the Structure Ranking Phase of CCDC 7th CSP Blind Test [29]. All lattice energies are per molecule basis in kJ/mol.

Model	CCDC 7th CSP Blind Test Polymorphs							
	Lattice Energy MAE [kJ/mol]	RMSE [kJ/mol]	r ²	Rank correlation Kendall	Spearman	Structures RMSD [Å]	RMSD st [Å]	Match rate
UMA								
UMA-S	2.69	3.67	0.73	0.82	0.93	0.12	0.07	0.99
UMA-M	2.66	3.71	0.60	0.81	0.91	0.13	0.07	0.99
UMA-L	2.49	3.70	0.81	0.84	0.95	0.12	0.07	1.00
Baselines								
eSEN-S-OMC	6.18	7.38	0.07	0.74	0.87	0.18	0.08	0.91

E.5 Molecular Crystals

Open Molecular Crystals (OMC25) [23] evaluates whether a model can predict the packing of molecule into crystal structures. This task requires the accurate estimation of inter-molecular forces. Results on validation and test splits are shown in Table 20. It is notable that all sizes of UMA models outperform the eSEN-S-OMC model trained on only OMC25. This indicates that the other datasets, such as OMol25, provide useful complementary information for the task. One important and real-world task for molecular crystals is to predict the lowest energy packing, called a polymorph, for a molecule. Results for this task for a subset of molecular crystal polymorphs from the most recent 7th Crystal Structure Prediction (CSP) Blind Test [29] are shown in Table 21. The pymatgen’s [52] StructureMatcher class with default settings is used to match DFT and UMA-relaxed polymorphs, and root mean square deviation (RMSD) is computed for matches. Similar to the test metrics, the UMA models outperform the eSEN-S-OMC trained on only OMC25.

E.6 Metal–Organic Frameworks

Table 22: OpenDAC [67] val and test table. All energies are in meV and forces are in meV/Å.

Model	Val (Total Energy)			Test (Ads. Energy)					
	Energy	Forces	Force Cosine	ID		OOD-LT			
				Energy	Forces	Force Cosine	Energy	Forces	Force Cosine
UMA									
UMA-S	60.4	5.9	0.82	169.5	16.7	0.63	292.4	16.0	0.57
UMA-M	59.3	3.8	0.91	167.3	14.8	0.62	290.2	10.7	0.76
UMA-L	38.7	3.3	0.91	177.1	7.8	0.82	291.1	6.5	0.91
Literature									
eqV2-ODAC [67]	-	-	-	145.0	8.2	0.69	316.0	7.2	0.72

The results on OpenDAC [67] are shown in Table 22. The OpenDAC dataset contains Metal-Organic Frameworks (MOFs) with CO₂ and water molecules. The goal is to estimate the change in energy in the presence with and without the CO₂ and water molecules. These adsorption energies are computed in the same manner as for catalysts. The use of total energies leads to significantly better adsorption

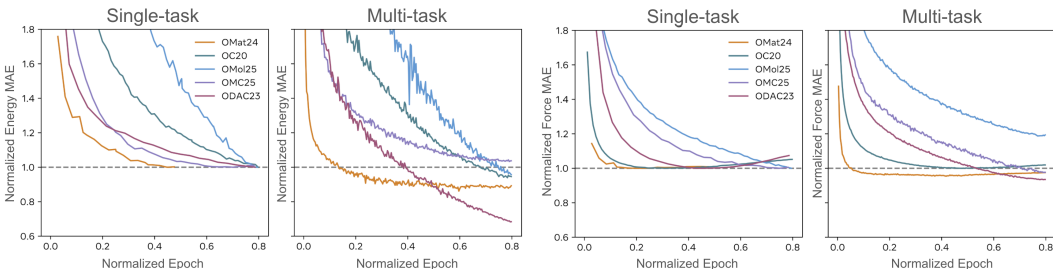


Figure 4: Pre-training curves of UMA-L for both single-task and multi-task models. Errors are normalized based on single-task performance. Note single-task models can overfit (forces on right), and the multi-task model generally converges to lower errors.

energy estimates, similar to catalysis. The forces of UMA-M and UMA-L are similar to the SOTA eqV2-ODAC [67] model.

F Single-task vs Multi-task

For large models, multi-task training offers benefits even without MoLE. In Figure 4, we plot the direct-force pre-training curves of UMA-Ig and single-task models with the same model architecture and size. All metrics are normalized to those achieved with the models trained on single tasks to easily compare their relative performance with multi-task models. We observe that single task models frequently overfit to forces (OMat overfits upon further training), while the multi-task UMA model does not. Furthermore, UMA achieves lower losses in most cases. The one exception is OMol forces, for which errors are already small ($< 10 \text{ meV}/\text{\AA}$) for both models.

G Additional MoLE Analysis

G.1 Expert Analysis

Using a limited validation set consisting of 10,000 OMat24, 5,000 OC20, 20,000 OMol25, 10,000 OMC25, and 5,000 ODAC23 samples, we calculate the mean expert coefficient for each element-expert pair across all systems where the pair appears. We visualize these results using 32 periodic tables, each representing one of the 32 experts in UMA-S (Figure 5).

Additionally we visualize the expert coefficient mean and variance across datasets (tasks). Many experts utilized in OC20 are also used in OMat24. In contrast, the experts associated with OMol25 show minimal overlap with other datasets, aside from a small subset shared with OM25C. Lastly ODAC23 and OMC25 utilize the fewest experts, and these two share a single expert between them.

G.2 Generalization Across Architectures

Table 23: Testing the generalization capability of MoLE layers. We applied 8-expert MoLE layers to both eSEN[21] and EquiformerV2[44] model architectures and measured their relative performance on direct pretraining against the versions without no MoLE. For each row, we show the relative improvement over the baseline.

OMol25 Val subset	eSEN 6M	EquiformerV2 6M
Metal Complexes	+10%	+10%
Spice	+5%	+5%
Neutral organics	0%	+3%
Biomolecules	+25%	+21%
Electrolytes	+12%	+10%
Mean across subsets	+10%	+10%

We performed additional analysis to ablate the benefit of the MoLE layers. Since our MoLE implement is very general and can be applied any linear layers inside a model, we ran experiments adding MoLE

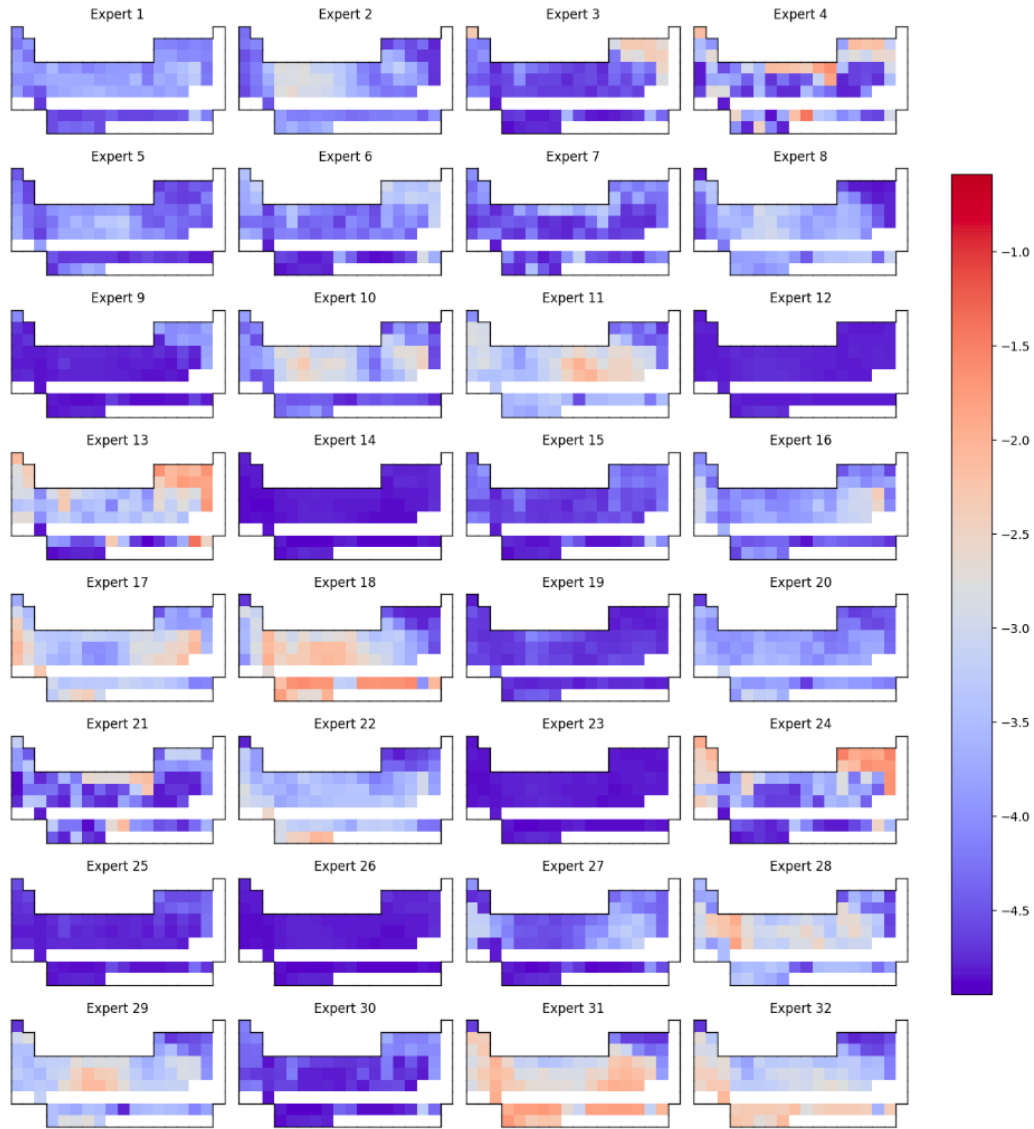


Figure 5: Log mean expert coefficient across element-expert pairs.

to both eSEN and EquiformersV2 architectures, controlling for model size (6M base parameters) and 8 training epochs on Omol dataset, direct pretraining only.

23 shows that despite EquiformersV2 and eSEN being very different architectures, the relative benefit of adding MoLE is fairly consistent in both cases. This suggests that MoLE is a simple and general approach to boost the capacity of MLIP models without incurring inference speed and memory overhead.

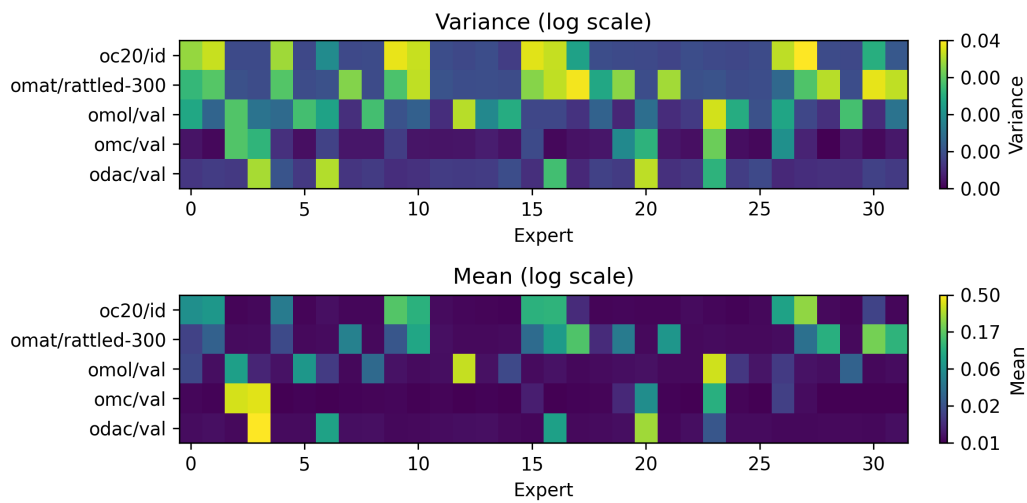


Figure 6: Log mean expert coefficient across element-expert pairs.

NeurIPS Paper Checklist

The checklist is designed to encourage best practices for responsible machine learning research, addressing issues of reproducibility, transparency, research ethics, and societal impact. Do not remove the checklist: **The papers not including the checklist will be desk rejected.** The checklist should follow the references and follow the (optional) supplemental material. The checklist does NOT count towards the page limit.

Please read the checklist guidelines carefully for information on how to answer these questions. For each question in the checklist:

- You should answer [Yes], [No], or [NA].
- [NA] means either that the question is Not Applicable for that particular paper or the relevant information is Not Available.
- Please provide a short (1–2 sentence) justification right after your answer (even for NA).

The checklist answers are an integral part of your paper submission. They are visible to the reviewers, area chairs, senior area chairs, and ethics reviewers. You will be asked to also include it (after eventual revisions) with the final version of your paper, and its final version will be published with the paper.

The reviewers of your paper will be asked to use the checklist as one of the factors in their evaluation. While "[Yes]" is generally preferable to "[No]", it is perfectly acceptable to answer "[No]" provided a proper justification is given (e.g., "error bars are not reported because it would be too computationally expensive" or "we were unable to find the license for the dataset we used"). In general, answering "[No]" or "[NA]" is not grounds for rejection. While the questions are phrased in a binary way, we acknowledge that the true answer is often more nuanced, so please just use your best judgment and write a justification to elaborate. All supporting evidence can appear either in the main paper or the supplemental material, provided in appendix. If you answer [Yes] to a question, in the justification please point to the section(s) where related material for the question can be found.

IMPORTANT, please:

- **Delete this instruction block, but keep the section heading “NeurIPS Paper Checklist”.**
- **Keep the checklist subsection headings, questions/answers and guidelines below.**
- **Do not modify the questions and only use the provided macros for your answers.**

1. Claims

Question: Do the main claims made in the abstract and introduction accurately reflect the paper’s contributions and scope?

Answer: [Yes]

Justification: The main claims made in the abstract and introduction accurately reflect the paper’s contributions and scope. The abstract provides a short summary of the innovations and key findings presented in the paper, while the introduction outlines the research problem, objectives, and the significance of the work. Both sections are aligned with the results discussed in the subsequent sections of the paper.

Guidelines:

- The answer NA means that the abstract and introduction do not include the claims made in the paper.
- The abstract and/or introduction should clearly state the claims made, including the contributions made in the paper and important assumptions and limitations. A No or NA answer to this question will not be perceived well by the reviewers.
- The claims made should match theoretical and experimental results, and reflect how much the results can be expected to generalize to other settings.
- It is fine to include aspirational goals as motivation as long as it is clear that these goals are not attained by the paper.

2. Limitations

Question: Does the paper discuss the limitations of the work performed by the authors?

Answer: [Yes]

Justification: We discuss some of the limitations of our work in the discussion section, including long-range interactions and incorporation of charge and spin.

Guidelines:

- The answer NA means that the paper has no limitation while the answer No means that the paper has limitations, but those are not discussed in the paper.
- The authors are encouraged to create a separate "Limitations" section in their paper.
- The paper should point out any strong assumptions and how robust the results are to violations of these assumptions (e.g., independence assumptions, noiseless settings, model well-specification, asymptotic approximations only holding locally). The authors should reflect on how these assumptions might be violated in practice and what the implications would be.
- The authors should reflect on the scope of the claims made, e.g., if the approach was only tested on a few datasets or with a few runs. In general, empirical results often depend on implicit assumptions, which should be articulated.
- The authors should reflect on the factors that influence the performance of the approach. For example, a facial recognition algorithm may perform poorly when image resolution is low or images are taken in low lighting. Or a speech-to-text system might not be used reliably to provide closed captions for online lectures because it fails to handle technical jargon.
- The authors should discuss the computational efficiency of the proposed algorithms and how they scale with dataset size.
- If applicable, the authors should discuss possible limitations of their approach to address problems of privacy and fairness.
- While the authors might fear that complete honesty about limitations might be used by reviewers as grounds for rejection, a worse outcome might be that reviewers discover limitations that aren't acknowledged in the paper. The authors should use their best judgment and recognize that individual actions in favor of transparency play an important role in developing norms that preserve the integrity of the community. Reviewers will be specifically instructed to not penalize honesty concerning limitations.

3. Theory assumptions and proofs

Question: For each theoretical result, does the paper provide the full set of assumptions and a complete (and correct) proof?

Answer: [NA]

Justification: [NA]

Guidelines:

- The answer NA means that the paper does not include theoretical results.
- All the theorems, formulas, and proofs in the paper should be numbered and cross-referenced.
- All assumptions should be clearly stated or referenced in the statement of any theorems.
- The proofs can either appear in the main paper or the supplemental material, but if they appear in the supplemental material, the authors are encouraged to provide a short proof sketch to provide intuition.
- Inversely, any informal proof provided in the core of the paper should be complemented by formal proofs provided in appendix or supplemental material.
- Theorems and Lemmas that the proof relies upon should be properly referenced.

4. Experimental result reproducibility

Question: Does the paper fully disclose all the information needed to reproduce the main experimental results of the paper to the extent that it affects the main claims and/or conclusions of the paper (regardless of whether the code and data are provided or not)?

Answer: [Yes]

Justification: We describe the architecture, especially the novel features, in detail as part of the main text. We provide descriptions of the training procedure and the datasets used in main text with additional details in the appendix. For established evaluations we cite the standard procedure and if the evaluation is new we describe it. These cover the main components needed to reproduce the main results of the paper.

Guidelines:

- The answer NA means that the paper does not include experiments.
- If the paper includes experiments, a No answer to this question will not be perceived well by the reviewers: Making the paper reproducible is important, regardless of whether the code and data are provided or not.
- If the contribution is a dataset and/or model, the authors should describe the steps taken to make their results reproducible or verifiable.
- Depending on the contribution, reproducibility can be accomplished in various ways. For example, if the contribution is a novel architecture, describing the architecture fully might suffice, or if the contribution is a specific model and empirical evaluation, it may be necessary to either make it possible for others to replicate the model with the same dataset, or provide access to the model. In general, releasing code and data is often one good way to accomplish this, but reproducibility can also be provided via detailed instructions for how to replicate the results, access to a hosted model (e.g., in the case of a large language model), releasing of a model checkpoint, or other means that are appropriate to the research performed.
- While NeurIPS does not require releasing code, the conference does require all submissions to provide some reasonable avenue for reproducibility, which may depend on the nature of the contribution. For example
 - (a) If the contribution is primarily a new algorithm, the paper should make it clear how to reproduce that algorithm.
 - (b) If the contribution is primarily a new model architecture, the paper should describe the architecture clearly and fully.
 - (c) If the contribution is a new model (e.g., a large language model), then there should either be a way to access this model for reproducing the results or a way to reproduce the model (e.g., with an open-source dataset or instructions for how to construct the dataset).
 - (d) We recognize that reproducibility may be tricky in some cases, in which case authors are welcome to describe the particular way they provide for reproducibility. In the case of closed-source models, it may be that access to the model is limited in some way (e.g., to registered users), but it should be possible for other researchers to have some path to reproducing or verifying the results.

5. Open access to data and code

Question: Does the paper provide open access to the data and code, with sufficient instructions to faithfully reproduce the main experimental results, as described in supplemental material?

Answer: [Yes]

Justification: All code and data will be available upon publication.

Guidelines:

- The answer NA means that paper does not include experiments requiring code.
- Please see the NeurIPS code and data submission guidelines (<https://nips.cc/public/guides/CodeSubmissionPolicy>) for more details.
- While we encourage the release of code and data, we understand that this might not be possible, so “No” is an acceptable answer. Papers cannot be rejected simply for not including code, unless this is central to the contribution (e.g., for a new open-source benchmark).
- The instructions should contain the exact command and environment needed to run to reproduce the results. See the NeurIPS code and data submission guidelines (<https://nips.cc/public/guides/CodeSubmissionPolicy>) for more details.

- The authors should provide instructions on data access and preparation, including how to access the raw data, preprocessed data, intermediate data, and generated data, etc.
- The authors should provide scripts to reproduce all experimental results for the new proposed method and baselines. If only a subset of experiments are reproducible, they should state which ones are omitted from the script and why.
- At submission time, to preserve anonymity, the authors should release anonymized versions (if applicable).
- Providing as much information as possible in supplemental material (appended to the paper) is recommended, but including URLs to data and code is permitted.

6. Experimental setting/details

Question: Does the paper specify all the training and test details (e.g., data splits, hyperparameters, how they were chosen, type of optimizer, etc.) necessary to understand the results?

Answer: [Yes]

Justification: We provide full details about the training procedure, hyperparameters, datasets, and evaluations in the appendix.

Guidelines:

- The answer NA means that the paper does not include experiments.
- The experimental setting should be presented in the core of the paper to a level of detail that is necessary to appreciate the results and make sense of them.
- The full details can be provided either with the code, in appendix, or as supplemental material.

7. Experiment statistical significance

Question: Does the paper report error bars suitably and correctly defined or other appropriate information about the statistical significance of the experiments?

Answer: [No]

Justification: Given the computational expense, we did not train ensembles of models.

Guidelines:

- The answer NA means that the paper does not include experiments.
- The authors should answer "Yes" if the results are accompanied by error bars, confidence intervals, or statistical significance tests, at least for the experiments that support the main claims of the paper.
- The factors of variability that the error bars are capturing should be clearly stated (for example, train/test split, initialization, random drawing of some parameter, or overall run with given experimental conditions).
- The method for calculating the error bars should be explained (closed form formula, call to a library function, bootstrap, etc.)
- The assumptions made should be given (e.g., Normally distributed errors).
- It should be clear whether the error bar is the standard deviation or the standard error of the mean.
- It is OK to report 1-sigma error bars, but one should state it. The authors should preferably report a 2-sigma error bar than state that they have a 96% CI, if the hypothesis of Normality of errors is not verified.
- For asymmetric distributions, the authors should be careful not to show in tables or figures symmetric error bars that would yield results that are out of range (e.g. negative error rates).
- If error bars are reported in tables or plots, The authors should explain in the text how they were calculated and reference the corresponding figures or tables in the text.

8. Experiments compute resources

Question: For each experiment, does the paper provide sufficient information on the computer resources (type of compute workers, memory, time of execution) needed to reproduce the experiments?

Answer: [Yes]

Justification: We provide details about the resources used for training our main family of models (small, medium, large) in the appendix. This includes a breakdown of the various training stages.

Guidelines:

- The answer NA means that the paper does not include experiments.
- The paper should indicate the type of compute workers CPU or GPU, internal cluster, or cloud provider, including relevant memory and storage.
- The paper should provide the amount of compute required for each of the individual experimental runs as well as estimate the total compute.
- The paper should disclose whether the full research project required more compute than the experiments reported in the paper (e.g., preliminary or failed experiments that didn't make it into the paper).

9. Code of ethics

Question: Does the research conducted in the paper conform, in every respect, with the NeurIPS Code of Ethics <https://neurips.cc/public/EthicsGuidelines?>

Answer: [Yes]

Justification: We respect the NeurIPS code of Ethics and do our best to preserve anonymity.

Guidelines:

- The answer NA means that the authors have not reviewed the NeurIPS Code of Ethics.
- If the authors answer No, they should explain the special circumstances that require a deviation from the Code of Ethics.
- The authors should make sure to preserve anonymity (e.g., if there is a special consideration due to laws or regulations in their jurisdiction).

10. Broader impacts

Question: Does the paper discuss both potential positive societal impacts and negative societal impacts of the work performed?

Answer: [Yes]

Justification: We discuss the positive societal impact in the introduction/results and discuss potential misuse and how that risk is mitigated in the discussion.

Guidelines:

- The answer NA means that there is no societal impact of the work performed.
- If the authors answer NA or No, they should explain why their work has no societal impact or why the paper does not address societal impact.
- Examples of negative societal impacts include potential malicious or unintended uses (e.g., disinformation, generating fake profiles, surveillance), fairness considerations (e.g., deployment of technologies that could make decisions that unfairly impact specific groups), privacy considerations, and security considerations.
- The conference expects that many papers will be foundational research and not tied to particular applications, let alone deployments. However, if there is a direct path to any negative applications, the authors should point it out. For example, it is legitimate to point out that an improvement in the quality of generative models could be used to generate deepfakes for disinformation. On the other hand, it is not needed to point out that a generic algorithm for optimizing neural networks could enable people to train models that generate Deepfakes faster.
- The authors should consider possible harms that could arise when the technology is being used as intended and functioning correctly, harms that could arise when the technology is being used as intended but gives incorrect results, and harms following from (intentional or unintentional) misuse of the technology.
- If there are negative societal impacts, the authors could also discuss possible mitigation strategies (e.g., gated release of models, providing defenses in addition to attacks, mechanisms for monitoring misuse, mechanisms to monitor how a system learns from feedback over time, improving the efficiency and accessibility of ML).

11. Safeguards

Question: Does the paper describe safeguards that have been put in place for responsible release of data or models that have a high risk for misuse (e.g., pretrained language models, image generators, or scraped datasets)?

Answer: [Yes]

Justification: The model will have appropriate terms of use when released.

Guidelines:

- The answer NA means that the paper poses no such risks.
- Released models that have a high risk for misuse or dual-use should be released with necessary safeguards to allow for controlled use of the model, for example by requiring that users adhere to usage guidelines or restrictions to access the model or implementing safety filters.
- Datasets that have been scraped from the Internet could pose safety risks. The authors should describe how they avoided releasing unsafe images.
- We recognize that providing effective safeguards is challenging, and many papers do not require this, but we encourage authors to take this into account and make a best faith effort.

12. Licenses for existing assets

Question: Are the creators or original owners of assets (e.g., code, data, models), used in the paper, properly credited and are the license and terms of use explicitly mentioned and properly respected?

Answer: [No]

Justification: We have cited any assets used (to the best of our ability), but we do not explicitly state the license and terms of use for every asset.

Guidelines:

- The answer NA means that the paper does not use existing assets.
- The authors should cite the original paper that produced the code package or dataset.
- The authors should state which version of the asset is used and, if possible, include a URL.
- The name of the license (e.g., CC-BY 4.0) should be included for each asset.
- For scraped data from a particular source (e.g., website), the copyright and terms of service of that source should be provided.
- If assets are released, the license, copyright information, and terms of use in the package should be provided. For popular datasets, paperswithcode.com/datasets has curated licenses for some datasets. Their licensing guide can help determine the license of a dataset.
- For existing datasets that are re-packaged, both the original license and the license of the derived asset (if it has changed) should be provided.
- If this information is not available online, the authors are encouraged to reach out to the asset's creators.

13. New assets

Question: Are new assets introduced in the paper well documented and is the documentation provided alongside the assets?

Answer: [Yes]

Justification: When we introduce new assets such as data/code/models we make sure they are well documented. Upon publication, we plan to include URLs to access all new assets including detailed license information. These have not been included in the initial submission due to the difficulty in remaining anonymous.

Guidelines:

- The answer NA means that the paper does not release new assets.

- Researchers should communicate the details of the dataset/code/model as part of their submissions via structured templates. This includes details about training, license, limitations, etc.
- The paper should discuss whether and how consent was obtained from people whose asset is used.
- At submission time, remember to anonymize your assets (if applicable). You can either create an anonymized URL or include an anonymized zip file.

14. **Crowdsourcing and research with human subjects**

Question: For crowdsourcing experiments and research with human subjects, does the paper include the full text of instructions given to participants and screenshots, if applicable, as well as details about compensation (if any)?

Answer: [NA]

Justification: [NA]

Guidelines:

- The answer NA means that the paper does not involve crowdsourcing nor research with human subjects.
- Including this information in the supplemental material is fine, but if the main contribution of the paper involves human subjects, then as much detail as possible should be included in the main paper.
- According to the NeurIPS Code of Ethics, workers involved in data collection, curation, or other labor should be paid at least the minimum wage in the country of the data collector.

15. **Institutional review board (IRB) approvals or equivalent for research with human subjects**

Question: Does the paper describe potential risks incurred by study participants, whether such risks were disclosed to the subjects, and whether Institutional Review Board (IRB) approvals (or an equivalent approval/review based on the requirements of your country or institution) were obtained?

Answer: [NA]

Justification: [NA]

Guidelines:

- The answer NA means that the paper does not involve crowdsourcing nor research with human subjects.
- Depending on the country in which research is conducted, IRB approval (or equivalent) may be required for any human subjects research. If you obtained IRB approval, you should clearly state this in the paper.
- We recognize that the procedures for this may vary significantly between institutions and locations, and we expect authors to adhere to the NeurIPS Code of Ethics and the guidelines for their institution.
- For initial submissions, do not include any information that would break anonymity (if applicable), such as the institution conducting the review.

16. **Declaration of LLM usage**

Question: Does the paper describe the usage of LLMs if it is an important, original, or non-standard component of the core methods in this research? Note that if the LLM is used only for writing, editing, or formatting purposes and does not impact the core methodology, scientific rigor, or originality of the research, declaration is not required.

Answer: [NA]

Justification: [NA]

Guidelines:

- The answer NA means that the core method development in this research does not involve LLMs as any important, original, or non-standard components.
- Please refer to our LLM policy (<https://neurips.cc/Conferences/2025/LLM>) for what should or should not be described.